AD-A151 701

HIGH SPECIFIC POWER AIRCRAFT TURN
MANEUVERS: TRADEOFF OF TIME-TO-TURN
VERSUS CHANGE IN SPECIFIC ENERGY

THESIS

AFIT/GAE/AA/78D-5   STEVEN B. DRON
CAPT   USAF

DTIC
S
E
MAR 28 1985
D

DEPARTMENT OF THE AIR FORCE
AIR UNIVERSITY (ATC)

AIR FORCE INSTITUTE OF TECHNOLOGY

Wright-Patterson Air Force Base, Ohio

85   03   13   085

HIGH SPECIFIC POWER AIRCRAFT TURN
MANEUVERS: TRADEOFF OF TIME-TO-TURN
VERSUS CHANGE IN SPECIFIC ENERGY

THESIS

AFIT/GAE/AA/78D-5   STEVEN B. DRON
CAPT   USAF

MAR 28 1985

HIGH SPECIFIC POWER AIRCRAFT TURN
MANEUVERS: TRADEOFF OF TIME-TO-TURN
VERSUS CHANGE IN SPECIFIC ENERGY

THESIS

Presented to the Faculty of the School of Engineering
of the Air Force Institute of Technology
Air Training Command
in Partial Fulfillment of the
Requirements for the Degree of
Master of Science

by

Steven B. Dron, B.S.
Capt   USAF

Graduate Aerospace Engineering
September 1984

Preface

This work is the result of my attempt during course work at and after separation from AFIT to define a tradeoff between time-to-turn and final specific energy for an aircraft with high specific power. I am indebted to Capt James Rader, my thesis advisor for getting me started, to Mr. Elisha Rachovitsky and Mr. Gerald M. Anderson for their encouragement and advice and to my family and friends for their continued moral support. Special thanks are in order for my wife, Lucy, who has admirably withstood these past seven years, and to the Trinity, for the Light in this age of Darkness. Amen

Steven B. Dron

Table of Contents

List of Figures

List of Tables

Abstract

The report deals with a tradeoff between time-to-turn and the change in specific energy during a turn of 180°, for an aircraft of high specific power. This type of aircraft possesses the capability to sustain flight at the corner velocity where the aircraft flies at maximum lift coefficient and maximum load factor simultaneously. However, the classical necessary conditions breakdown on this corner velocity arc and an addition constraint set must be defined to determine the optimal control histories. The report first defines the necessary conditions for a generic optimal control formulation with two state-dependent inequality constraints and then applies the formulation to a high specific power aircraft problem. The result is a three-point boundary value problem including a discontinuous interior corner time at the beginning of sustained corner velocity flight. All state and costate derivatives and end conditions are presented with numerical methods for determining minimum time, maximum energy and maximum energy gradient solutions. Anticipated results are provided for the formulations beginning at initial conditions both above and below the corner velocity. Results are presented for the minimum time solution only. Recommendations for further work in this same area are also provided.

HIGH SPECIFIC POWER AIRCRAFT TURN
MANEUVERS: TRADEOFF OF TIME-TO-TURN
VERSUS CHANGE IN SPECIFIC ENERGY

I. INTRODUCTION

Since World War I, great strides have been made in
the field of energy management of combat aircraft. Most
of the presently used tactics were developed during the
early portion of this century, but their detailed
explanation and simulation has only been accomplished in
the past 25 years. As more progress is made in aircraft
design and capabilities, new avenues of research in
energy management are opened for examination.

Much work has been done in the areas of fuel and
energy management for fighter aircraft of the 1960's thru
1970's vintage, particularly the area of minimum time-to-
turn. In research of any particular aircraft's minimum-
time turn performance, a solution is sought whereby the
angle of attack, bank angle and throttle histories create
an exchange of potential and kinetic energy to produce
the highest turn rate possible at all points in time.
For every aircraft, there is a velocity which is a
function of altitude, at which the maximum possible turn
rate occurs. It is that airspeed at which maximum lift
coefficient and maximum load factor occur simulataneously
and it is known as the corner velocity. Beginning at a
particular initial airspeed and altitude, flying as close
as possible to this velocity at all times gives the
minimum time turn for that aircraft.

Historically, aircraft have possessed excessive weight and induced drag and insufficient thrust to sustain flight at their corner velocities although they can instantaneously pass through this condition during a maximum performance maneuver. However, as technology advances, lighter, more aerodynamically efficient aircraft with increased thrust are developed which can more closely approximate sustained corner velocity flight.

In the near future, fighter aircraft may produce more than the minimum required specific power to sustain corner velocity flight and will be able to achieve the maximum possible turning rate at less than maximum throttle setting. Should this capability exist for a particular aircraft, it would be of interest to examine the tradeoff between time allotted to complete a 180° velocity vector heading change and the resultant specific energy change at the end of the turn, for turns that begin both below and above the corner velocity. The examination of this tradeoff and the set of optimal control histories which produce it is the objective of this thesis.

This work is an extension of the work done by Humphreys (Ref 5) and Anderson (Ref 1). In this effort, the aircraft model of Humphreys and the kinematic optimal control equations developed by Anderson are blended with desired initial and final flight conditions to form a

2

pair of Three Point Boundary Value Problems (TPBVP); one
for minimum time (free final time) and one for maximum
energy gain (fixed final time). From these formulations,
the tradeoff is determined.

II. Statement of the Problem

Connection of Energy and Time in a Turn

As stated in the introduction, the objective of this thesis is to examine the tradeoff between time to complete a 180° velocity vector heading change and the resultant specific energy change from the beginning of the turn to the end. Therefore, the tradeoff criterion between energy and time must be defined.

The total energy of an aircraft is the sum of its potential and kinetic energy components and can be stated as:

$$E_T = mgh + \tfrac{1}{2}mV^2 \qquad\qquad (2-1)$$

which has units of foot-pounds. The specific energy, or the energy altitude of an aircraft is the total energy per pound of aircraft weight and can be expressed as:

$$E = h + \frac{V^2}{2g} \qquad\qquad (2-2)$$

which has units of feet. If an aircraft begins a turn with some initial specific energy, E_i, the effects of climbing and diving, drag and thrust application will transition the initial aircraft energy state to a final energy state, E_f, in a time, t_f.

For a minimum time turn, energy is sacrificed for the sake of continuous maximum turn rate. In this case, the final energy E_{min} will be the lowest final energy of any

of the turns to be examined and it will occur at a time t_{min}, the minimum time to turn to the final conditions. If the time allotted to turn is increased to $t_f > t_{min}$, then the opportunity exists to perform the same turn in a more energy conscious manner and therefore, $E_f > E_{min}$. The more time allotted for the turn, the more energy can be conserved or gained.

Definition of the Tradeoff

It is postulated that a final specific energy, E_{trade}, occurring at a final time t_{trade} will maximize the specific energy gradient defined as:

$$EG = \frac{E_f - E_i}{t_f} \qquad (2-3)$$

E_{trade}, t_{trade} and EG_{max} can be graphically or numerically determined by a line, eminating from E_i at $t=0$ being placed tangent to a final specific energy versus final time plot. This is qualitatively shown in Fig 2-1. An additional method for determining EG_{max} is to plot the energy gradient versus final time and pick the maximum value. This can be seen from Fig 2-2.

The determination of t_{trade}, E_{trade} and therefore EG_{max} for turns beginning at equal specific energy states, both below and above the corner velocity, is the goal of this effort. This could be done using a single problem formulation, such as maximize EG, instead of

5
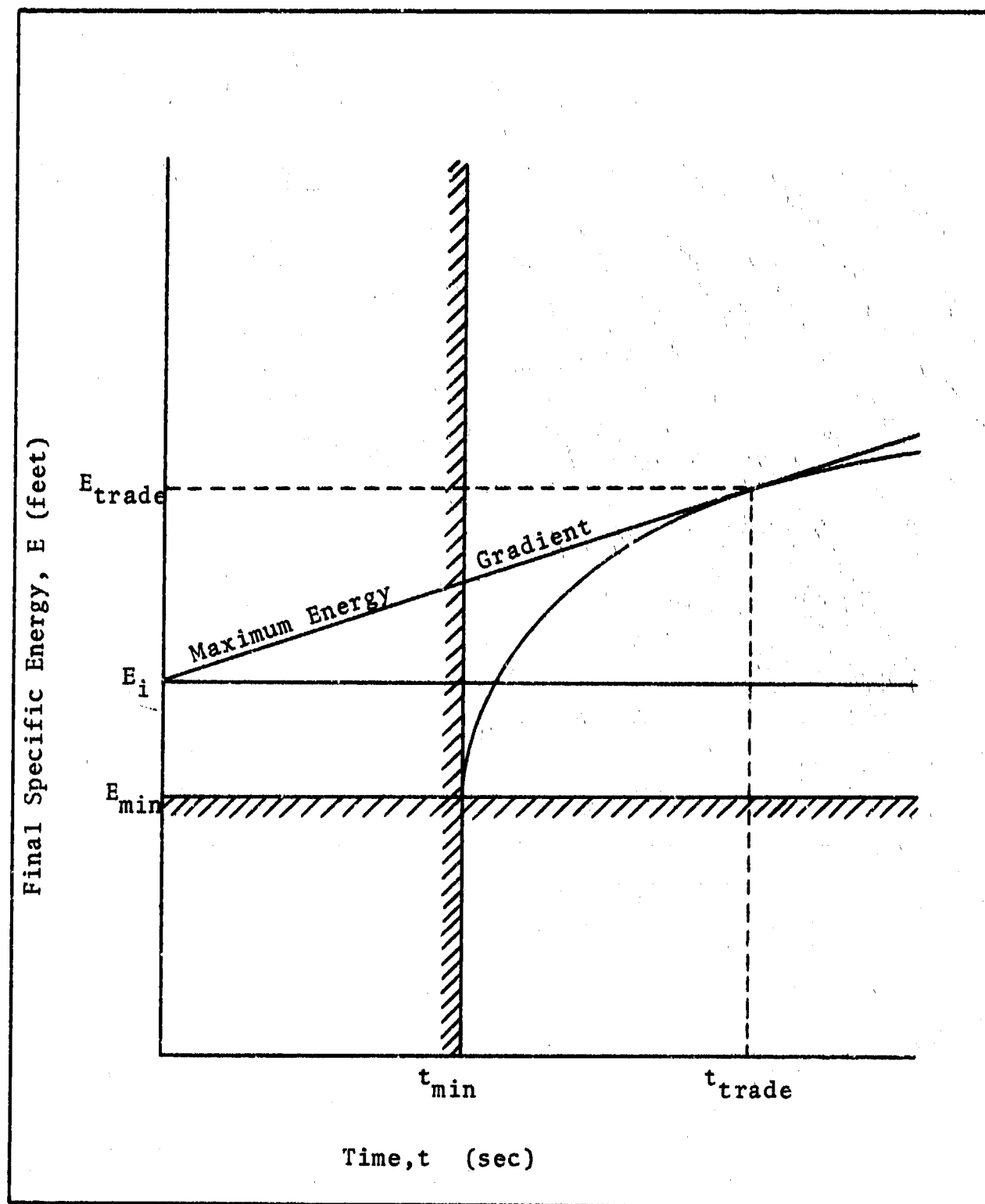
Figure 2-1. Final Specific Energy vs. Time-to-Turn
depicting the Maximum Energy Gradient
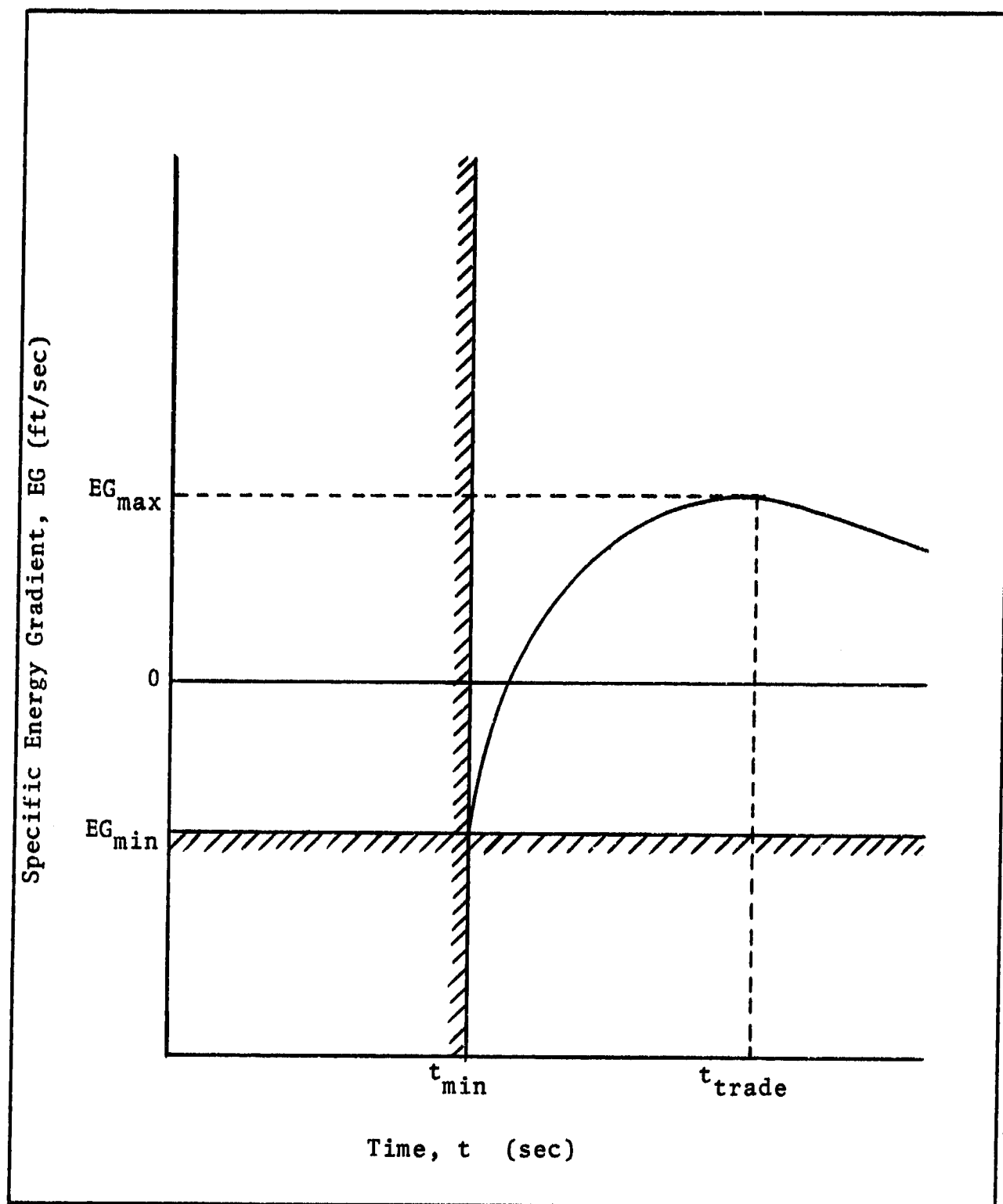
Figure 2-2. Specific Energy Gradient vs. Time-to-Turn
depicting EG_{max}.

defining a minimum time turn and several maximum energy turns, but it would not be as useful a result for comparative purposes as the formulation chosen. This method unambiguously determines the time-energy tradeoff.

III. Generic Optimal Control Formulation

The system to be optimally controlled will be represented by the dynamic differential system (Ref 1)

$$\dot{x} = f(x,u,t) \qquad (3\text{-}1)$$

with initial and final time conditions

$$x(t_O) = x_O \; , \; K\left[x(t_f),t_f\right] = 0 \qquad (3\text{-}2)$$

Both x and $\dot{x}$ are n-dimensional state vectors, u is an m-dimensional control vector, K is an s-dimensional vector of final conditions and t represents time. The problem objective is to transfer the system from the initial conditions to the final conditions while minimizing the Bolza form payoff function

$$J = G\left[x(t_f),t_f\right] + v^T K\left[x(t_f),t_f\right]$$

$$+ \int_{T_\bullet}^{T_f} \left[F(x,u,t) + \lambda^T(f-\dot{x})\right] dt \qquad (3\text{-}3)$$

G is a scalar function of final time and final time state conditions and F is a scalar integral function subject to state and control values and time. The vector v^T is an s-dimensional constant Lagrange multiplier vector, and λ^T is an n-dimenional Lagrange multiplier costate vector otherwise known as the influence function vector. The Hamiltonian is expressed as:

$$H(x,u,t) = F(x,u,t) + \lambda^T f(x,u,t) \qquad (3\text{-}4)$$

The control vector, u, is subject to both non-state-dependent and state-dependent inequality constraints. The non-state dependent constraints do not affect the control formulation, only the control vector bounds. They will be considered separately in section 4. For the class of problems discussed here, it is postulated that the ith element of the control vector is subject to two state-dependent inequality constraints

$$C_1(x,u_i,t) \leq 0, \quad C_2(x,u_i,t) \leq 0 \tag{3-5}$$

Adjoining these constraints to the Hamiltonian, it becomes

$$H = F(x,u,t) + \lambda^T f(x,u,t) + \mu_1 C_1(x,u_i,t)$$
$$+ \mu_2 C_2(x,u_i,t) \tag{3-6}$$

where μ_1 and μ_2 are scalar Lagrange multipliers. The conditions on μ_1 and μ_2 are

$$\begin{aligned} \mu_j &= 0 \text{ if } C_j(x,u_i,t) \leq 0 \\ \mu_j &\neq 0 \text{ if } C_j(x,u_i,t) = 0 \end{aligned} \quad j=1,2 \tag{3-7}$$

if, and only if, both C_1 and C_2 are not both zero simultaneously. If only one constraint is zero at any time, applying the Euler-Lagrange optimality condition,

$$H_u = 0 \tag{3-8}$$

produces the impulse response functions and the non-zero value of μ_j can be found from the relationship

10

$$H_{u_i} = F_{u_i} + \lambda^T f_{u_i} + \mu_j C_j u_i = 0 \qquad j = 1,2 \qquad (3\text{-}9)$$

However, if both state-dependent inequality constraints are zero simultaneously, Eq (3-9) becomes

$$H_{u_i} = F_{u_i} + \lambda^T f_{u_i} + \mu_1 C_1 u_i + \mu_2 C_2 u_i = 0 \qquad (3\text{-}10)$$

as Eq (3-10) is the only equation which yields values for μ_1 or μ_2, unique solutions for μ_1 and μ_2 cannot be obtained with one equation and two unknowns, and alternate solution must be sought.

The solution selected is to form a new state dependent equality constraint from both C_1 and C_2 simultaneously equaling zero (Ref 1:182, 2:2247, 3:117). This new constraint has the form

$$S(x,t) = 0 \qquad (3\text{-}11)$$

However, this constraint is not explicitly a function of the control vector and the optimal controls cannot be found from this expression. Using the techniques of (Ref 3:118), it is found that the qth time derivative of Eq (3-11) produces a constraint containing elements of the control vector. This new constraint

$$S^{(q)}(x,u,t) = 0 \qquad (3\text{-}12)$$

is known as a singular arc and may now be adjoined to Eq (3-6) to form the new Hamiltonian

11

$$H = F(x,u,t) + \lambda^T f(x,u,t) + \mu_1 C_1(x,u_i,t)$$
$$+ \mu_2 C_2(x,u_i,t) + \mu_3 S^{(q)}(x,u,t) \quad (3\text{-}13)$$

For this new formulation, it should be understood that Eqs (3-7) are still valid if only one constraint is zero at a time. If both C_1 and C_2 are zero simultaneously, then Eq (3-11) is satisfied and μ_1 and μ_2 are defined to both be zero. The unique value for μ_3 is determined by applying Eq (3-8) to Eq (3-13) which produces

$$H_u = F_u + \lambda^T f_u + \mu_3 S_u^{(q)} = 0 \quad (3\text{-}14)$$

In addition to the singular arc constraint, q interior point constraints have been generated which must be adhered to at the beginning and end of the arc, and are represented in vector form as

$$M = \left[S, \dot{S}, \ldots S^{(q-1)} \right] = 0 \quad (3\text{-}15)$$

The Hamiltonian, H, and the costate variables, λ^T are discontinuous at the beginning of the arc, but continuous at the end (Ref 2:2248). If the discontinuity, or corner, happens at time t_c, then the shifts in the values of H and λ^T are the differences between their values just before and after t_c and can be expressed as

$$H(t_c^-) = H(t_c^+) - \eta^T M_t \Big|_{t\,=\,t_c} \quad (3\text{-}16)$$

$$\lambda^T(t_c^-) = \lambda^T(t_c^+) + \eta^T M_x \Big|_{t\,=\,t_c} \quad (3\text{-}17)$$

where η^T is a q-dimensional constant Lagrange multiplier

12

vector. The values of η^T are found by simultaneously solving Eq (3-16) and Eq (3-17).

In summary, given the system and conditions of Eqs (3-1) and (3-2), the payoff function of Eq (3-3) becomes

$$J = G + \upsilon^T K$$

$$+ \int_{T_0}^{T_f} \left[F + \lambda^T(f-\dot{x}) + \mu^T\left(C_1,C_2,S^{(q)}\right) \right] dt \quad (3-17)$$

and the Hamiltonian is expressed by Eq (3-12). The optimal controls are found by applying Eq (3-8) to Eq (3-13) subject to the constraints of Eqs (3-7), those following Eq (3-13), and insuring satisfaction of the Legendre-Clebsch condition

$$H_u{}^T{}_u \geq 0 \quad (3-18)$$

The costate differential equations equal $-H_x$ and are

$$\dot{\lambda}^T = -(F_x + \lambda^T f_x + \mu_1 C_{1_x} + \mu_2 C_{2_x} + \mu_3 S_x{}^{(q)}) \quad (3-19)$$

Application of the transversality conditions yield the final time values of the costates and Hamiltonian to be

$$\lambda^T(t_f) = G_x\left[x(t_f),t_f\right] + \upsilon^T K_x\left[x(t_f),t_f\right] \quad (3-20)$$

$$H(t_f) = -G_t\left[x(t_f),t_f\right] - \upsilon^T K_t\left[x(t_f),t_f\right] \quad (3-21)$$

which completes formation of the three point boundary value problem (TPBVP). Eq (3-21) applies only to the free final time problem. The interior point constraints of Eq (3-15) and the corner discontinuities of Eq (3-16)

and Eq (3-17) must also be satisfied when switching onto or off of the singular arc of Eq (3-12) at the corner time, t_c.

IV. Specific Optimal Control Formulation

Point Mass Aircraft System Definition

To satisfy Eq (3-1), the aircraft for both minimum time and maximum final energy turn problems will be represented by the following point mass equations of motion (Ref 12)

$$\dot{x} = V \cos\gamma \cos\psi \qquad (4\text{-}1a)$$

$$\dot{Y} = V \cos\gamma \sin\psi \qquad (4\text{-}1b)$$

$$\dot{h} = V \sin\gamma \qquad (4\text{-}1c)$$

$$\dot{V} = g\left[\frac{T\pi - D}{W} - \sin\gamma\right] \qquad (4\text{-}1d)$$

$$\dot{\gamma} = \frac{g}{V}\left[\frac{L}{W}\cos\phi - \cos\gamma\right] \qquad (4\text{-}1e)$$

$$\dot{\psi} = \frac{g}{V\cos\gamma}\left[\frac{L}{W}\sin\phi\right] \qquad (4\text{-}1f)$$

The variables x, y and h form the three axis position, V is velocity, γ is the flight path angle and ψ is the heading angle. T is the constant maximum available thrust, D is drag, L is lift, W is a constant weight and g is the acceleration of gravity. The expressions for lift and drag are

$$L = \tfrac{1}{2}\rho_0 \sigma V^2 A C_L \qquad (4\text{-}2a)$$

$$D = \tfrac{1}{2}\rho_0 \sigma V^2 A (C_{D_0} + k C_L^2) \qquad (4\text{-}2b)$$

where A is the reference wing area, C_L is the lift coefficient, C_{D_0} is the zero lift drag coefficient and k is the induced drag parameter. The parameter $\rho_0 \sigma$ is the exponential air density expression

15

$$\rho_o \sigma = \rho_o e^{\beta(h-h_D)} \tag{4-3a}$$

where β is a constant and h_D is the minimum altitude of interest. Least squares curve fits to data from atmospheric tables (Ref 8) produce

$$\rho_o \sigma_T = 0.0023769 e^{-\left[\frac{h}{30477}\right]} \tag{4-3b}$$

$$\rho_o \sigma_s = 0.00072736 e^{-\left[\frac{h-36089}{20953}\right]} \tag{4-3c}$$

Where Eqs (4-3b) and (4-3c) represent the troposphere and stratosphere respectively. For this exercise, only Eq (4-3b) will be employed due to the altitudes at which the aircraft maneuvers will be examined.

The control vector is

$$u = \begin{bmatrix} \phi & C_L & \pi \end{bmatrix} \tag{4-4}$$

where ϕ is the bank angle, C_L is the lift coefficient and π is the throttle setting. The constraints on the control vector are

$$-180^\circ \leq \phi \leq +180^\circ \tag{4-5a}$$

$$C_1 = (C_L - C_{L_{max}}) \leq 0 \tag{4-5b}$$

$$C_2 = (C_L - \frac{2WN_{max}}{\rho_o V^2 A \sigma}) \leq 0 \tag{4-5c}$$

$$C_3 = C_L \geq 0 \tag{4-5d}$$

$$-0.5 \leq \pi \leq 1.0 \tag{4-5e}$$

where $C_{L_{max}}$ is the maximum aerodynamic lift coefficient and N_{max} is the maximum allowable normal load factor.

From Eq (4-3) it is seen that the bank angle is unbounded, the lift coefficient must always be greater than zero, less than both the maximum aerodynamic lift coefficient and that for achieving maximum load factor and the throttle setting may vary from half reverse thrust to full forward thrust settings.

High Specific Power Aircraft - Corner Velocity Constraint

If both Eqs (4-5b,c) are simultaneously zero, Eq (3-11) is formed and is

$$S(x,t) = \sigma V^2 - \frac{2WN_{max}}{\rho_o A C_{L_{max}}} = 0 \qquad (4-6)$$

This expression must be satisfied if sustained maximum turn rate flight at the corner velocity is to be part of the optimal trajectory. However, it is readily seen that Eq (4-6) is not explicitly a function of any control and therefore successive time derivatives must be taken until Eq (3-12) is formed. This equation is

$$\dot{S}(x,t) = V^2 \sigma_h \dot{h} + 2 \sigma V \dot{V} = 0 \qquad (4-7)$$

Substitution of Eq (4-1c,d) into Eq (4-7) and rearranging the resultant expression yields

$$\dot{S}(x,u,t) = g \left[\frac{T\pi - D}{W} - \sin\gamma \left(1 - \beta \frac{V^2}{2g}\right) \right] = 0 \qquad (4-8)$$

This expression is a function of throttle setting and lift coefficient and satisfies the requirements of Eq (3-

12). Therefore, only one interior point constraint exists, Eq (4-6), and Eq (3-15) becomes

$$M = S(x,t) = \sigma V^2 - \frac{2WN_{max}}{\rho_0 A C_{L_{max}}} = 0 \qquad (4-9)$$

The Hamiltonian of Eq (3-13) can now be formed and is

$$H = \lambda_x \dot{x} + \lambda_y \dot{y} + \lambda_h \dot{h} + \lambda_v \dot{V} + \lambda_\gamma \dot{\gamma} + \lambda_\psi \dot{\psi}$$
$$+ \mu_2 g(\frac{L}{W} - N_{max}) + \mu_3 g\left[\frac{T\pi - D}{W} - \sin\gamma(1 - \beta\frac{V^2}{2g})\right] \quad (4-10)$$

For this type of aircraft problem, there is no integral function $F(x,u,t)$ and the constraint C_1 of Eq (4-5b) is not state dependent and need not be adjoined to the Hamiltonian. Neither M nor H is explicitly a function of time and therefore from Eq (3-16) it is seen that

$$M_t \Big| t=t_c = 0 \quad \therefore \ H(t_c^-) = H(t_c^+) \qquad (4-11)$$

$$H_t = 0 \ \therefore \ H(t_o) = H(t_c) = H(t_f) = constant \quad (4-12)$$

Recalling Eq (3-17) and applying Eq (4-9), it is seen that only λ_h and λ_v will have interior point discontinuities which are

$$\lambda_h(t_c^-) = \lambda_h(t_c^+) + \eta\beta\sigma V^2 \qquad (4-13a)$$

$$\lambda_v(t_c^-) = \lambda_v(t_c^+) + 2\eta\sigma V \qquad (4-13b)$$

Upon substitution of Eq (4-13) into Eq (4-11) it is found that

$$\eta = - \frac{\lambda_V{}^+}{2V\sigma} \qquad\qquad (4\text{-}14)$$

Resubstitution of Eq (4-14) into Eq (4-13) produces

$$\lambda_h(t_c{}^-) = \lambda_h(t_c{}^+) - \lambda_v(t_c{}^+)\frac{\beta V}{2} \qquad (4\text{-}15a)$$

$$\lambda_v(t_{\bar{c}}) = 0 \qquad\qquad (4\text{-}15b)$$

The discontinuity in λ_v and the dependence of $\lambda_h(t_c{}^-)$ on $\lambda_v(t_c{}^+)$ makes forward integration of the differential equations impossible and backward integration from the final conditions to the initial conditions is required. This will be discussed in Sec 5.

Optimal Controls

The optimal controls are defined by applying the Euler-Lagrange condition, Eq (3-8) and the Legendre - Clebsch condition, Eq (3-18) to the Hamiltonian of Eq (4-10). To find the optimal bank angle, ϕ , two equations must be satisfied. They are

$$H_\phi = \lambda_\gamma \frac{g}{V} \frac{L}{W}(-\sin \phi) + \frac{g}{V\cos\gamma}\lambda_\psi \frac{L\cos\phi}{W} = 0 \quad (4\text{-}16a)$$

or

$$H_\phi = -\lambda_\gamma \sin\phi + \lambda_\psi \frac{\cos\phi}{\cos\gamma} = 0 \qquad\qquad (4\text{-}16b)$$

and

$$H_{\phi\phi} = -\lambda_\gamma \cos\phi - \lambda_\psi \frac{\sin\phi}{\cos\gamma} \geq 0 \qquad\qquad (4\text{-}17)$$

In order for both of these conditions to be satisfied simultaneously, the only solution is

$$\cos\phi = \frac{\lambda_\gamma}{\sqrt{\lambda_\gamma{}^2 + \left(\frac{\lambda_\psi}{\cos}\right)^2}} \quad , \quad \sin\phi = -\frac{\lambda_\psi/\cos\gamma}{\sqrt{\lambda_\gamma{}^2 + \left(\frac{\lambda_\psi}{\cos}\right)^2}} \quad (4\text{-}18)$$

19

Upon substitution of the non-unique $\cos\phi$ and $\sin\phi$ expressions into Eq (4-17) it is seen that

$$H_{\phi\phi} = \pm\sqrt{\lambda_\gamma{}^2 + \left(\frac{\lambda_\psi}{\cos\gamma}\right)^2} \geq 0 \qquad (4-19)$$

thus insuring a minimizing control at all times. Eq. (4-18) will produce the optimal bank angle history.

To define the optimal lift coefficient, again two conditions must be adhered to. They are

$$H_{C_L} = -\frac{g}{W}\lambda_v D_{C_L} + \frac{g}{WV}\lambda_\gamma L_{C_L}\cos\phi + \frac{g\lambda_\psi}{WV\cos} L_{C_L}\sin\phi$$

$$+ \frac{g}{W}\mu_2 L_{C_L} - \frac{g}{W}\mu_3 D_{C_L} = 0 \qquad (4-20)$$

$$H_{C_L C_L} = -\frac{g}{W}\lambda_v D_{C_L C_L} - \frac{g}{W}\mu_3 D_{C_L C_L} \geq 0 \qquad (4-21)$$

Rearranging and substituting Eq (4-17) yields

$$H_{C_L} = -(\lambda_v + \mu_3)D_{CL} - (\frac{H_{\phi\phi}}{V} - \mu_2)L_{C_L} = 0 \qquad (4-22)$$

and

$$H_{C_L C_L} = -(\lambda_v + \mu_3)D_{C_L C_L} \geq 0 \qquad (4-23)$$

For an interior C_L control which is within the constraints of Eqs (4-5b,c,d) both μ_2 and μ_3 are zero. Therefore, Eq (4-23) states that for an optimum interior control

$$\lambda_v \leq 0 \qquad (4-24)$$

as $D_{C_L CL}$ is always positive. Eq (4-22) produces the optimum interior control

20

$$C_L = \frac{-H_{\phi\phi}}{2kV\lambda v} \tag{4-25}$$

If any of the bounds of Eq (4-5b,c,d) are exceeded by Eq (4-25), C_L is set to the boundary value exceeded. If maximum load factor flight occurs, Eq (4-5c) is zero, and the non-zero value of μ_2 is calculated from Eq (4-22) to be

$$\mu_2 = \frac{4kWN_{max}\lambda_v}{\rho_o \sigma V^2 A} + \frac{H_{\phi\phi}}{V} \tag{4-26}$$

To determine the condition of H_{C_L} during corner velocity flight, the throttle history must be examined first.

The two final equations which must be investigated for the optimal thrust control are

$$H_\tau = (\lambda v + \mu_3)g\frac{T}{W} = 0 \tag{4-27}$$

and

$$H_{\tau\tau} = 0 \tag{4-28}$$

Eqs (4-27) and (4-28) demonstrate that the throttle is a singular control because it does not appear in Eq (4-27). Therefore, unless μ_3 equals λv, which can only happen during sustained corner velocity flight, the throttle setting cannot be an interior value, but must be a minimum or maximum boundary value depending upon the value of λ_v. Using Eq (4-5e) and Eq(4-27) it is determined that

21

$$\pi = 1.0 \text{ for } \lambda_v < 0 \qquad\qquad (4\text{-}29a)$$

$$\pi = -0.5 \text{ for } \lambda_v > 0 \qquad\qquad (4\text{-}29b)$$

If λv equals zero, which happens as the corner velocity arc is entered as shown by Eq (4-15b), then the throttle value is determined to be

$$\pi = 1.0 \text{ for } \dot\lambda_v \geq 0 \qquad\qquad (4\text{-}30a)$$

$$\pi = -0.5 \text{ for } \dot\lambda_v \leq 0 \qquad\qquad (4\text{-}30b)$$

For flight along the corner velocity arc, the partial or interior throttle setting can be determined from Eq (4-8) to be

$$\pi = \frac{1}{T}\left[D_{max} + W \sin\gamma\,(1 - \beta\frac{V^2}{2g}) \right] \qquad\qquad (4\text{-}31)$$

For this interior control to be a viable solution, from Eq (4-27), it is seen that

$$\mu_3 = -\lambda v \qquad\qquad (4\text{-}32)$$

Upon substitution of Eq (4-32) into Eq (4-22), it is determined that along the corner velocity arc

$$H_{C_L} = -\frac{H\phi\phi L}{V}C_L \leq 0 \qquad\qquad (4\text{-}33)$$

as all of the components of H_{C_L} are always positive. Therefore, Eq (4-33) demands that $C_{L_{max}}$ be the optimum C_L for this condition which corroborates the requirements of Eq (4-6).

Costate Differential Equations

Of the three Euler-Lagrange conditions, two have been developed; one for the state derivatives of Eqs (3-1) and (4-1) and a second, Eq (3-8), to determine the minimizing optimal controls just discussed. The third condition, Eq (3-19), deals with the costate differential system, and produces the following equations:

$$\dot{\lambda}_x = 0 \tag{4-34}$$

$$\dot{\lambda}_y = 0 \tag{4-35}$$

$$\dot{\lambda}_h = \frac{g}{W}\left[D_h(\lambda_v + \mu_3) + L_h(\frac{H\phi\phi}{V} - \mu_2) \right] \tag{4-36}$$

$$\dot{\lambda}_v = \frac{g}{W}\left[D_v(\lambda_v + \mu_3) + L_v(\frac{H\phi\phi}{V} - \mu_2) \right]$$
$$+ \frac{1}{V}(\lambda_\gamma \dot{\gamma} + \lambda_\psi \dot{\psi}) - \sin\gamma(\lambda_h + \mu_3 \beta V)$$
$$- \cos\gamma(\lambda_x \cos\psi + \lambda_y \sin\psi) \tag{4-37}$$

$$\dot{\lambda}_\gamma = \sin\gamma\left[V(\lambda_x\cos\psi + \lambda_y \sin\psi) - \lambda_\gamma \frac{g}{V} \right]$$
$$+ \cos\gamma\left[g\left[\lambda_v + \mu_3(1 - \beta\frac{V^2}{2g}) \right] - \lambda_h V \right]$$
$$- \lambda_\psi \dot{\psi}\tan\gamma \tag{4-38}$$

$$\dot{\lambda}_\psi = V\cos\gamma(\lambda_x \sin\psi - \lambda_y \cos\psi) \tag{4-39}$$

Aircraft Model

The coefficients used to complete the point mass aircraft model are identical to those of (Ref 5:97). The quantities in table (4-1) were used to calculate the initial altitude and airspeed values of Table (4-2).

Name	parameter	value
Thrust, max	T	18,225 lbs*
Weight	W	12,150 lbs
Maximum load factor	Nmax	7.22
Reference Wing Area	A	237 ft^2
zero lift drag coefficient	c_{D_O}	0.02
induced drag coefficient	k	0.05
maximum lift coefficient	$c_{L_{max}}$	1.0

* - This thrust corresponds to T/W = 1.5

Table 4-1. Point Mass Aircraft Model Parameters

Transversality Conditions

As stated in Sec. 3, the transversality conditions, Eqs (3-20) and (3-21), complete the formation of the TPBVP. For the minimum time and maximum energy turns to be investigated, the state dependent conditions of Eq (3-2) are as shown in Table (4-2). From that table, it is evident that for all cases examined,

$$K \left[x(t_f), t_f \right] = \left[\begin{array}{c} \gamma \\ \psi - \pi \end{array} \right]_{t=t_f} \tag{4-40}$$

where π in this case represents 180° in radians.

24

Parameter	Symbol	End Conditions for $V_i < V_c$		End Conditions for $V_i > V_c$	
		initial*	final	initial*	final
Down Range Distance	X	0	—	0	—
Cross Range Distance	Y	0	—	0	—
Altitude	h	25,000 ft	—	15,000 ft	—
Velocity	V	527.8 fps	—	960.2 fps	—
Flight Path Angle	γ	0	0	0	0
Heading Angle	ψ	0	3.14159 RAD	0	3.14159 RAD

*NOTE: These initial conditions of altitude and velocity for turns beginning both above and below the corner velocity correspond to a specific energy of 29,329 ft. The corner velocity for this specific energy level is 774.8 fps at 20,000 ft. The initial conditions are equally offset from this corner velocity condition by ±5000 feet in altitude.

Table 4-2. Initial and Final Conditions for Minimum Time and Maximum Energy Problems

Employing Eq (3-20), it is determined that

$$\left[\lambda_x \ \lambda_y \ \lambda_h \ \lambda_v \ \lambda_\gamma \ \lambda_\psi \right] t=t_f = \left[0 \ 0 \ G_h \ G_v \ \nu_1 \ \nu_2 \right] \qquad (4\text{-}41)$$

which are not a function of the state final conditions, K. This result holds for all three problem formulations. It is noted that from Eqs (4-34), (4-35) and (4-41) that λ_x and λ_y are always zero, have no effect upon the problem solutions and may be eliminated from the formulations from here on. For simplification, Eq (4-39) now becomes

$$\dot{\lambda}_\psi = 0 \qquad (4\text{-}42)$$

Eq (4-41) shows that values for λ_h and λ_v at the final time can be explicitly calculated, but values for λ_γ and λ_ψ must be judiciously selected. No additional help can be provided for selecting initial guesses for the finals values of λ_γ and λ_ψ for a fixed final time problem; only that they together must generate a feasible final time bank angle.

However, for both free final time problems, using Eqs (3-13), (3-21), (4-8), (4-40) and (4-41), it can be shown that at $t = t_f$

$$\lambda_\gamma \dot{\gamma} + \lambda_\psi \dot{\psi} + G_{t_f} = 0 \qquad (4\text{-}43)$$

As noted in (Ref 1:183), when a singular arc of this type is part of the optimal trajectory, the trajectory terminates on the arc. This is helpful for two reasons:

1) the final velocity is the corner velocity and 2) the final load factor is maximum allowable load factor. Upon substitution of these two facts plus Eqs (4-1e,f), (4-17) (4-19) and quantities from table (4-2), it is seen that

$$\frac{gN}{V} \sqrt{\lambda_\gamma^2 + \lambda_\psi^2} + \lambda_\gamma \frac{g}{V} - G_{t_f} = 0 \qquad (4-44)$$

With one equation and two unknowns, one variable must be selected. To help make the best selection, two observations can be made: 1) based on Eq (4-40) a positive, right turn must be executed and 2) from Eqs (4-1f) and (4-18), a negative value of λ_ψ must exist to insure a right turn. Therefore, λ_γ shall be selected and λ_ψ calculated from the relationship

$$\lambda_\psi = -\sqrt{\left(\frac{V}{gN}\right)^2 \left(G_{t_f} - \frac{g}{V}\lambda_\gamma\right)^2 - \lambda_\gamma^2} \qquad (4-45)$$

To insure that a negative radical is not chosen λ_γ is limited by solving Eq (4-44) for λ_γ and substituting $\lambda_\psi = 0$. The result is

$$-G_{t_f}\frac{V}{g}\left|\frac{N+1}{N^2-1}\right| \leq \lambda_\gamma \leq G_{t_f}\frac{V}{g}\left|\frac{N-1}{N^2-1}\right| \qquad (4-46)$$

It is of interest to plot Eq (4-44) to aid in selecting a reasonable bank angle at the final time. Fig 4-1 is plotted as an example for a minimum time-to-turn problem

27
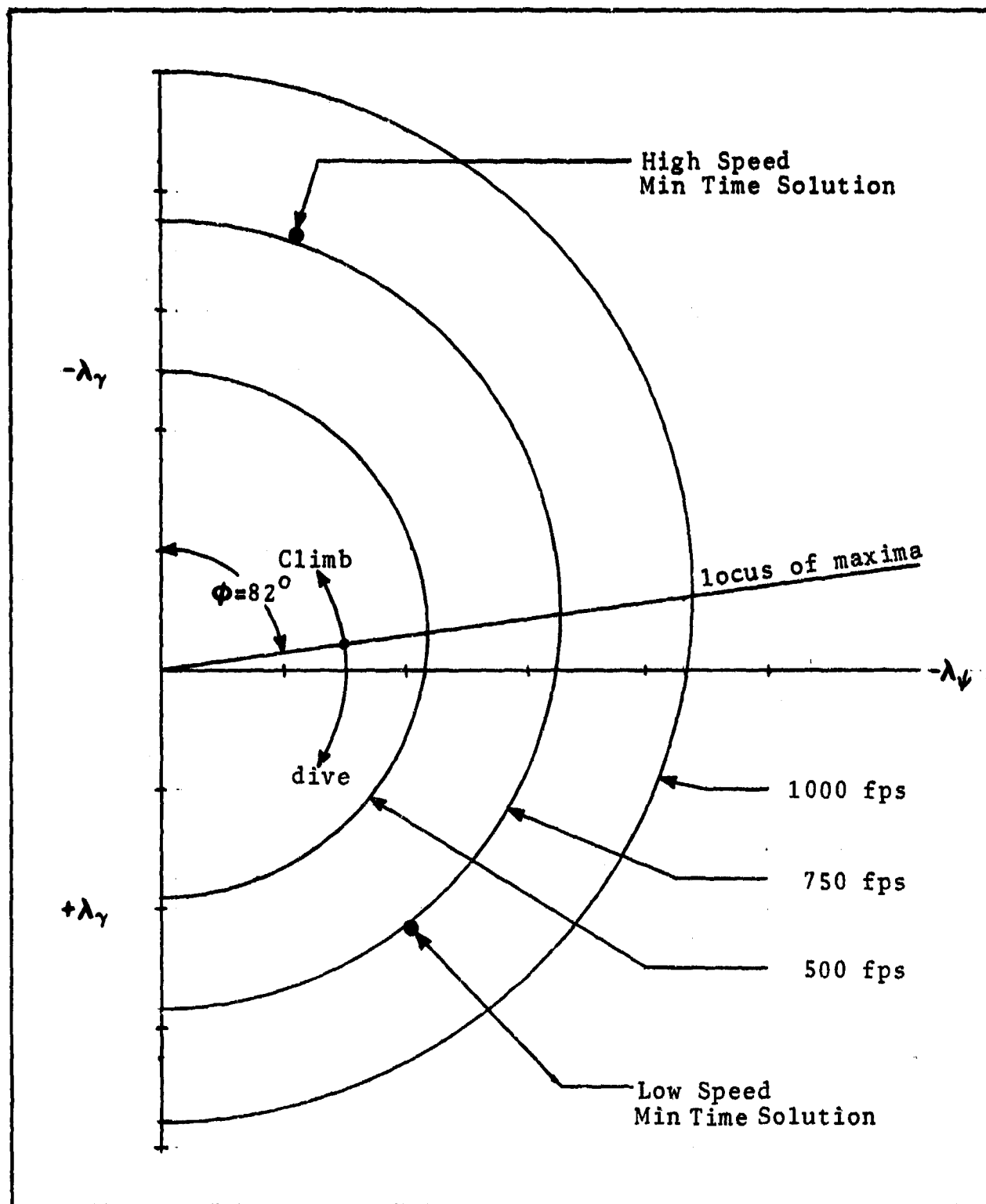
Figure 4-1. Minimum Time Final Velocity Contour Plot
for selection of λ_γ and λ_ψ

(G_{t_f}=1) for final velocities of 500, 750 and 1000 fps. As seen in the figure, there is a locus of maxima for all velocities which is a straight line. Solving Eq (4-44) for the value of λ_γ which maximizes λ_ψ yields.

$$\lambda_\gamma = \frac{-V}{g(N^2-1)} \quad , \quad \lambda_{\psi max} = \frac{-V}{g\sqrt{N^2-1}} . \qquad (4-47)$$

The values of Eq (4-47) in turn yield

$$\tan\phi = \sqrt{N^2-1} \qquad (4-48)$$

which is the tangent of the bank angle for a level coordinated turn at the final time. Note that the locus plotted corresponds to 82° of bank for 7.22g's only. Therefore, choosing combinations of λ_γ and λ_ψ above the locus will cause the aircraft to pitch up at t_f and combinations below it will cause a pitch down. A similar plot can be generated for any other free final time problem.

In summary, the costate final conditions are stated as follows:

a) minimum time

$$G = t_f \qquad \lambda = \begin{bmatrix} 0 & 0 & 0 & 0 & \lambda_\gamma & \lambda_\psi \end{bmatrix} \qquad (4-49)$$

b) maximum energy

$$G = E_i - E_f \qquad \lambda = \begin{bmatrix} 0 & 0 & -1 & \frac{-V}{g} & \lambda_\gamma & \lambda_\psi \end{bmatrix} \qquad (4-50)$$

29

c. maximum energy gradient

$$G = \frac{Ei-Ef}{t_f} \qquad \lambda = \begin{bmatrix} 0 & 0 & \dfrac{-1}{t_f} & \dfrac{-V}{gt_f} & \lambda_\gamma & \lambda_\psi \end{bmatrix} \qquad (4-51)$$

Substitution of table 4-1 quantities into Eq (4-6) yields

$$V_c = 558.07\sqrt{\frac{1}{\sigma}} \qquad (4-52)$$

From Eq (4-52), it is clear that the selection of a final altitude fixes the final velocity. Along with a choice for a final time, the values of λ_h and λ_V can be determined for all the problem formulations investigated.

For the selection of λ_γ and λ_ψ for fixed final time problems, arbitrary numbers which generate a feasible final bank angle are the best guesses. However, for free final time problems, use Eq (4-52) for a velocity, select a final bank angle for pitch up or pitch down at t_f, pick λ_γ off of Fig 4-1 using a protractor and substitute it into Eq (4-45) to calculate λ_ψ. This process will always insure that $H_f + G_{t_f} = 0$. The solutions for λ_γ and λ_ψ for both the high and low speed minimum time cases are plotted for reference on Fig 4-1.

Once these final conditions at t_f are established, the state and costate differential equations (4-1) and (4-34) through (4-39) can be integrated to the initial conditions at t_o. The methods of integration and search for the optimum control trajectory are covered in Sec 5.

V. Numerical Method for Solution of the TPBVP

As stated in Section 4, the dependence of λ_h^- and λ_v^- on λ_v^+ makes forward integration of the state and costate equations from initial to final conditions impossible. Backward integration from the final initial conditions must be employed for both minimum time and maximum energy problems.

Minimum Time-to-Turn TPBVP Solution

Given the 2n+1 dimensional final condition vector, Z_f, having the quantities

$$Z_f = \begin{bmatrix} X & Y & h & V & \gamma & \psi & \lambda_x & \lambda_y & \lambda_h & \lambda_v & \lambda_\gamma & \lambda_\psi & H \end{bmatrix}$$
$$= \begin{bmatrix} - & - & - & - & 0 & 180^\circ & 0 & 0 & 0 & 0 & \nu_1 & \nu_2 & -1 \end{bmatrix} \quad (5\text{-}1)$$

and the 2n+1 dimensional initial condition vector, Z_i, having the quantities

$$Z_i = \begin{bmatrix} X & Y & h & V & \gamma & \psi & \lambda_x & \lambda_y & \lambda_h & \lambda_v & \lambda_\gamma & \lambda_\psi & H \end{bmatrix}$$
$$= \begin{bmatrix} 0 & 0 & h_i & V_i & 0 & 0 & - & - & - & - & - & - & -1 \end{bmatrix} \quad (5\text{-}2)$$

two subset vectors relating final condition variables and initial condition requirements can be generated.

It can be seen from Eqs (4-1) and (4-34) through (4-39) and (4-41) that the down range and cross range variables X and Y and their respective influence functions λ_x and λ_y have no effect upon the problem solution as they are dependent variables. They can be eliminated from the solution for the sake of expediency.

It was learned from Sec 4 that a selection of the altitude at t_f dictated the final corner velocity. Therefore, velocity at t_f is no longer a variable. Additionally, the use of this altitude-velocity pair in concert with the requirement for $H_f + G_{t_f} = 0$ allowed for the calculation of λ_ψ at t_f as a function of λ_γ. Now, λ_ψ and H_f are no longer variables. As this is a free final time problem with an interior time constraint, t_f and t_c must be added as variables to be selected before the integration is performed. The final condition variable subset vector, z, which will be varied to reach the initial conditions is therefore

$$z = \begin{bmatrix} h & \lambda_\gamma & t_f & t_c \end{bmatrix} \qquad (5-3)$$

These four final time variables match with the four initial time requirements

$$z_i = \begin{bmatrix} h_i & V_i & \gamma_i & \psi_i \end{bmatrix} \qquad (5-4)$$

After integrating from the non-optimal z vector conditions at $t = t_f$ to $t = t_o$, there will be a non-zero residual miss vector R formed by the difference between the initial time results and the desired conditions. R is generated from z_i and is

$$R = \begin{bmatrix} h-h_i, & V-V_i, & \gamma, & \psi \end{bmatrix}_{t=t_o} \qquad (5-5)$$

32

The objective of the TPBVP is to select the variables in Z which when integrated from t_f to t_o drive the residual vector R to zero. In order to reduce the values in R from one iteration to the next, the direction and magnitude of the changes to the Z variable values must be determined. This can be done by solving a Taylor series expansion of R about the z vector. From (Ref 14:686), this is found to be

$$R(z + \delta z) = R(z) + \frac{\partial R}{\partial z} \delta z + \frac{1}{2} \delta z^T \frac{\partial^2 R}{\partial z^2} \delta z$$

$$+ \text{ Higher Order Terms} \qquad (5-6)$$

Assuming that the second and higher order terms in Eq (5-6) are negligible with respect to the first order term's influence on a solution, then the equation for change in R, ΔR, due to a variation in the final time vector z, δz, is

$$\Delta R = R(z + \delta z) - R(z) = \frac{\partial R}{\partial z} \delta z \qquad (5-7)$$

It is desirable that after a single variation of z, due to an increment δz, the term $R(z + \delta z)$ will diminish to zero. In order for a vector δz to be calculated which will cause $R(z + \delta z)$ to be zero, Eq (5-7) is modified to be

$$\Delta R = - R(z) = \frac{\partial R}{\partial z} \delta z \qquad (5-8)$$

Using Newton's Method of Tangents (Ref 6:170) to solve Eq (5-8) for δz, it is found that

$$\delta z = - \frac{\partial R}{\partial z}^{-1} R(z) \qquad (5-9)$$

R(z) is a straight-forward numerical difference as shown in Eq (5-5). The 4x4 first order derivative matrix is formed using a numerical central difference scheme (Ref 6:220) operating on each of the four variables in z. This is then inverted and used to calculate δz in Eq (5-9).

δz is the vector along which a search is conducted to find what fraction of its magnitude will cause the biggest reduction is the R(z) vector. Should a full magnitude search along δz not reduce the R vector on the first attempt, reductions in the magnitude of δz and subsequent searches are required until the maximum reduction in R is reached. The equation for reduction in δz is formed using the Golden Section Ration (Ref 6:460) and is

$$\delta z^{j+1} = 0.618034 \cdot \delta z^{j} \qquad j \geq 1 \qquad (5-10)$$

Reductions in δz are required until the maximum reduction in R is achieved.

In summary, the following steps are taken to obtain the optimal solution for the minimum time problem:

1) Select values for the elements of z which comply with the transversality conditions of Section 4.

2) Integrate the state and costate equations backwards constrained by the requirements of Section 4 from t_f through t_c to t_o and form the residual vector R.

3) Numerically form the derivative matrix $\frac{\partial R}{\partial z}$ by integrating backward to find the variations in R due to independent variations in the z elements.

4) Calculate δz from Eqs (5-9).

5) Modify the values of z by δz and perform a search.

6) If a reduction in R does not occur on this search, decrease δz according to Eq (5-10) and repeat step 5 until a reduction occurs.

7) If the root sum square (RSS) of elements of the reduced R vector is greater than 10^{-4}, then repeat steps 2 through 7.

8) If the RSS of R is less than 10^{-4}, then the solution has been achieved for the minimum time problem.

Maximum Energy Turn TPBVP Solution

The maximum energy turn formulation is nearly identical to the minimum time formulation. As Eq (4-43) does not apply to a fixed final time problem such as this, there are only 2n final conditions in the Z vector.

The resultant modifications to the z vector are that t_f is no longer a variable and λ_ψ has taken its place. This still leaves 4 variables and 4 equations to solve and the same methods used for solving for δz can be used.

Maximum Energy Gradient TPBVP Solution

The method used to solve this formulation is identical to the minimum time-to-turn method. Only the constant value for the Hamiltonian has changed due to the new values for G_{t_f}.

VI. Anticipated Results

No predictions for the values of t_{trade}, E_{trade} or EG_{max} can be made other than the qualitative predictions on Figures 2-1 and 2-2. However, qualitative predictions about the control histories can be presented. They are presented in Figures 6-1 through 6-6.

Optimal Control Histories

The predicted bank angle histories for $V_i > V_c$ are shown in Fig (6-1). For the minimum time turn (curve 'a'), an initial bank angle of less than 90° is required to climb while turning to bleed off airspeed as rapidly as possible. Subsequent to reaching the corner velocity arc, the bank angle is increased to be greater than 90° to restore the flight path angle end condition. Given more time in which to complete the turn, a slight decrease in the initial bank angle and a slight increase in final bank angle should be in order as climbing for a longer duration to a higher corner velocity should occur with resultant greater flight path angle excursions. However, the basic shape of the history should remain intact.

The lift coefficient histories shown in Fig (6-3) all represent maximum load factor flight until the corner velocity arc is encountered at which point $C_{L_{max}}$ is the optimum control. An interior lift coefficient may occur should time be available, and insufficient climb and acceleration capabilities exist at the higher altitudes

37

at the maximum load factor.

The throttle history for $V_i > V_c$ flight is the most provocative control to discuss for this problem. From (Ref 1), it is known that the throttle setting will be minimum until the corner velocity arc is intercepted at which point, an interior thrust control will be employed (curve 'a'). Given extra time to complete the turn and maximize the final energy it is postulated that the throttle will initially be at minimum setting and then switch for some time to maximum throttle prior to an interior corner velocity arc setting. This would be a "bang-bang-singular" throttle control (curve 'b'). This combination is proposed as it would require less power and time to decelerate from high speed and then reaccelerate to corner velocity arc than the converse. Given enough time, no minimum control bound would be expected; only maximum-singular control (curve 'c') as will be discussed for $V_i > V_c$.

For the case where $V_i < V_c$, the control histories should differ quite markedly from the $V_i > V_c$ case. In Fig (6-2), the initial bank angle for the minimum time turn, curve 'a', should be the largest of all the turns so as to create the greatest acceleration possible terminating in the smallest bank angle. Given more time to turn, (curve 'b'), less diving and more climbing would result, thus reducing the bank angle requirements. If sufficient time and excess power are available, the bank

angle may start at a value less than 90° and finish greater than 90° to maximize final altitude and airspeed.

The lift coefficient histories, as seen in Fig (6-4), should all be at maximum lift coefficient unless sufficient time to complete the turn is supplied wherein a corner velocity arc is not part of the optimal history. In that case, an interior lift coefficient may occur, but is not expected in this exercise.

From Fig (6-6), the throttle histories for $V_i < V_c$ all contain maximum throttle settings until the corner velocity arc is reached (curve 'a'), otherwise, known as "bang-singular" control. As time to turn is increased, climbing and accelerating to higher speeds should cause a larger t_c value and a higher corner arc throttle setting (curve 'b'). Given sufficient time to turn, a corner velocity arc may not be part of the optimal history and the result is a maximum throttle setting throughout the turn. The shape of the throttle history during corner velocity flight is dictated by an altitude rate and flight path angle rate combination.

None of the plots presented are intended to be construed as predictions of exact values in either time or control variable. They are intended to predict trends for comparisons between minimum time and maximum energy turns.
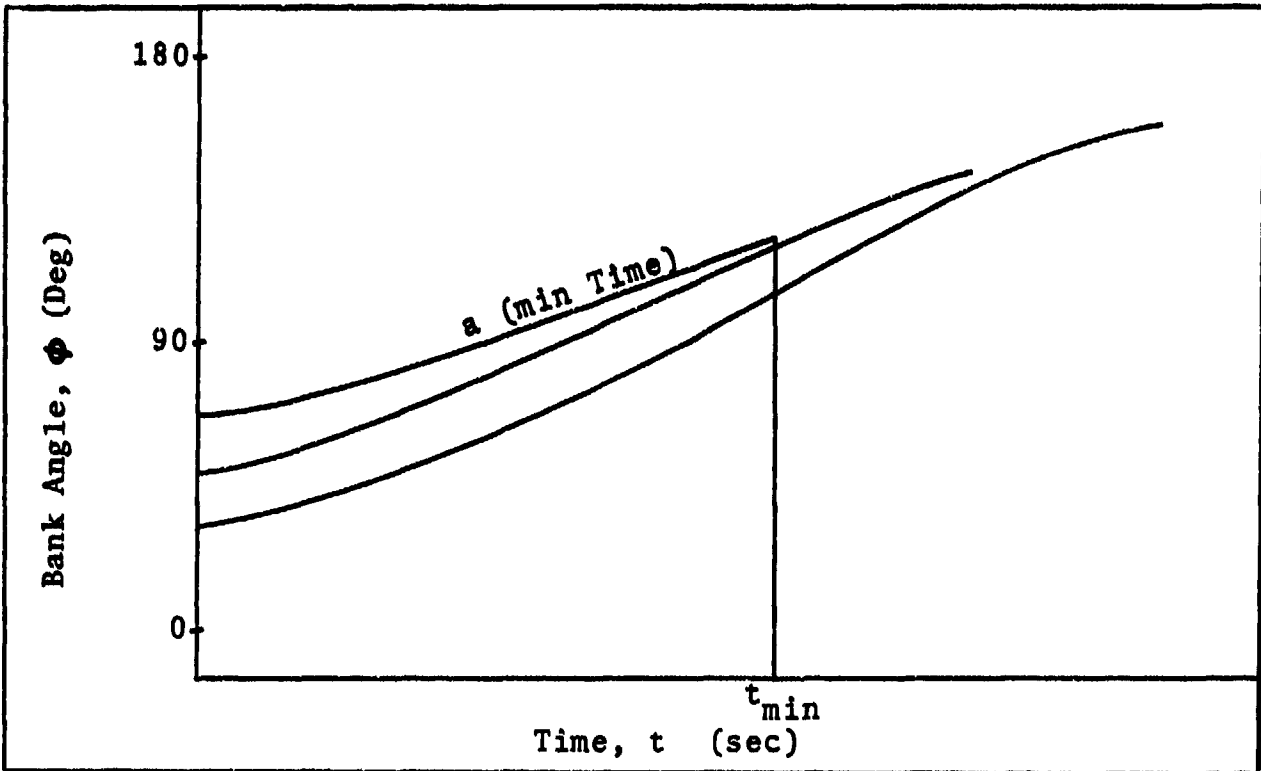
Figure 6-1.   Bank Angle vs. Time for $V_i > V_c$
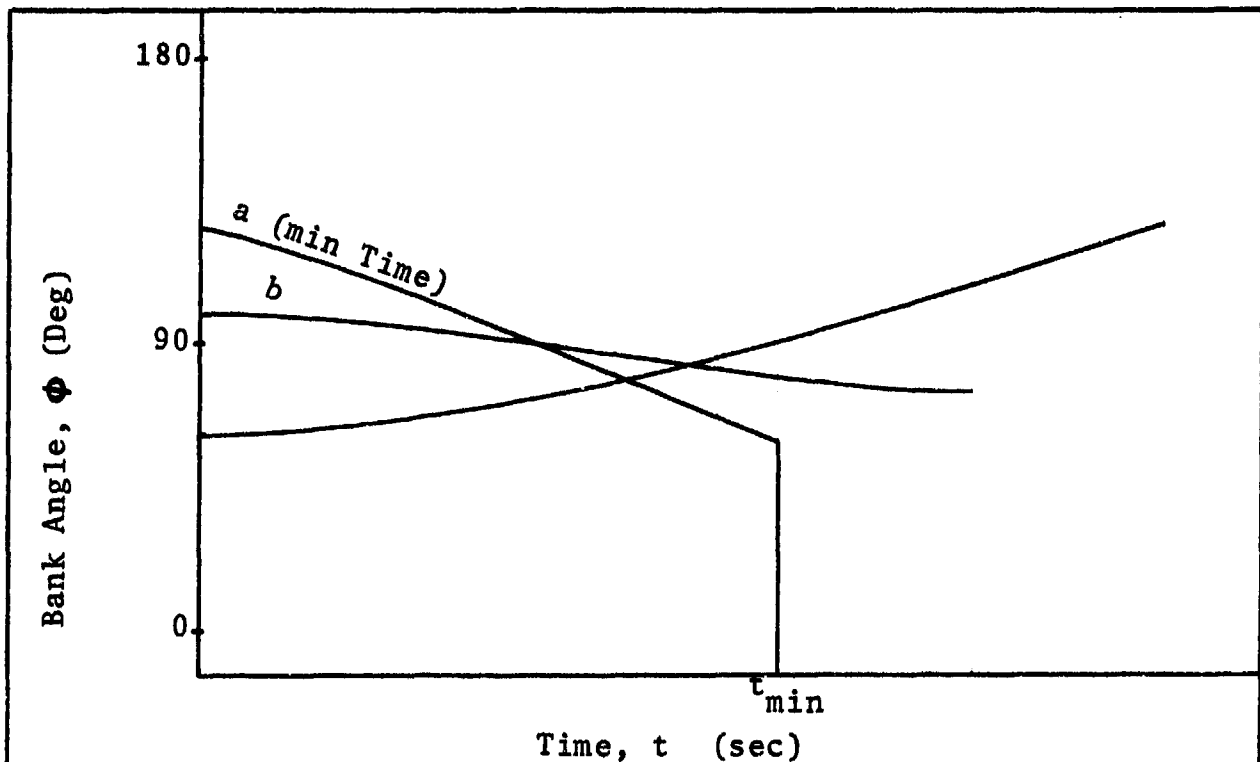
Figure 6-2.   Bank Angle vs. Time for $V_i < V_c$
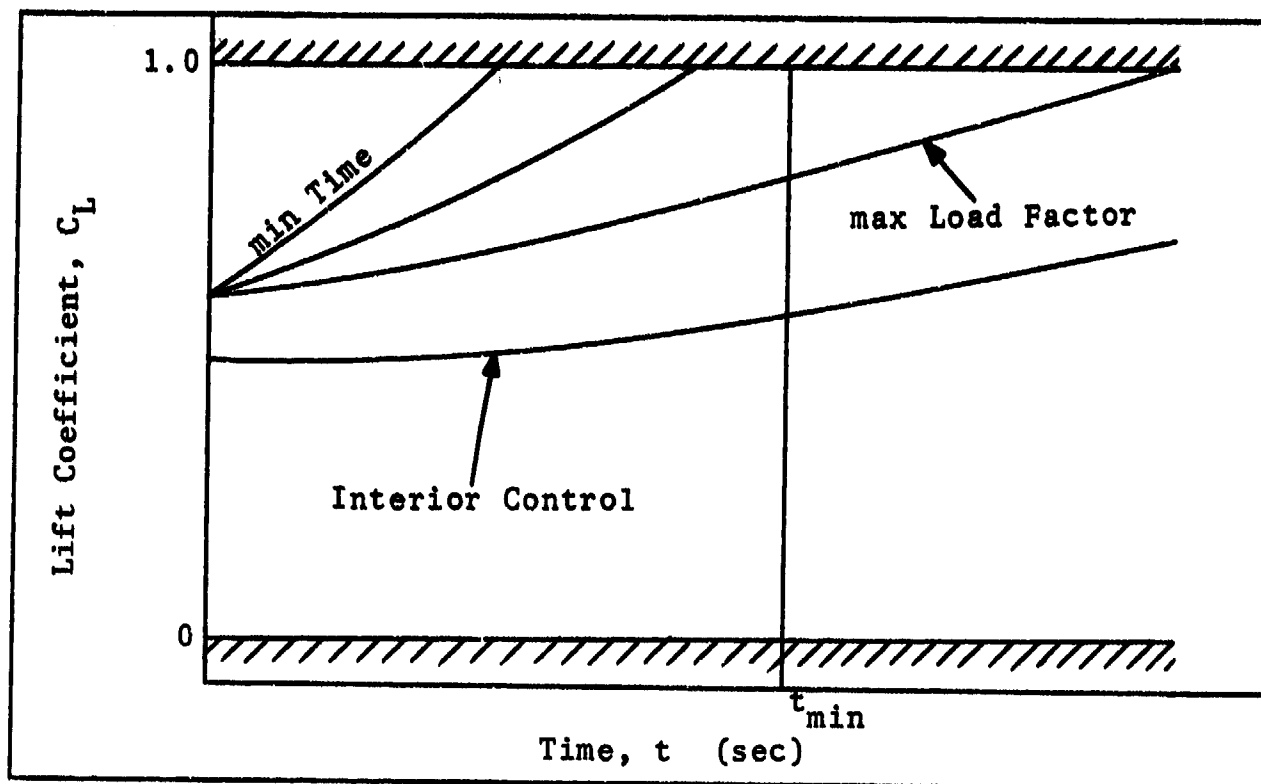
Figure 6-3.   Lift Coefficient vs. Time for $V_i > V_c$
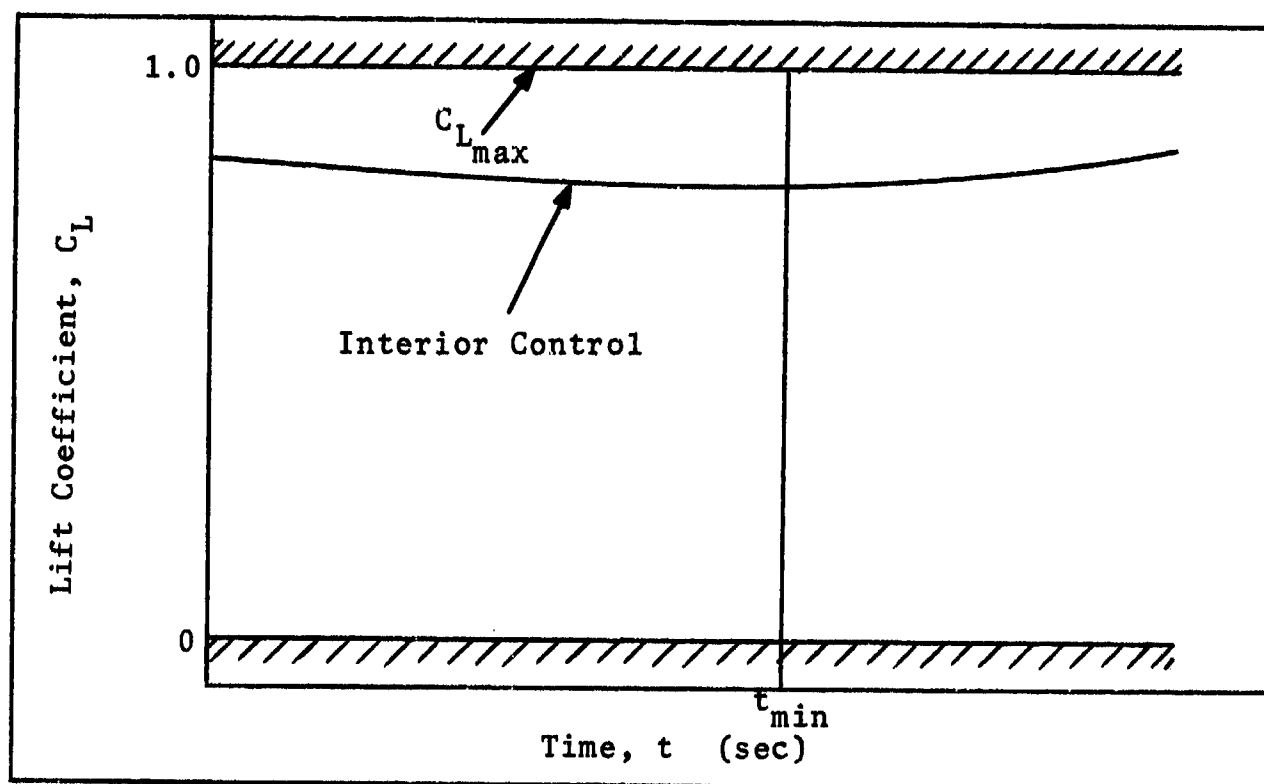
Figure 6-4.   Lift Coefficient vs. Time for $V_i < V_c$

41
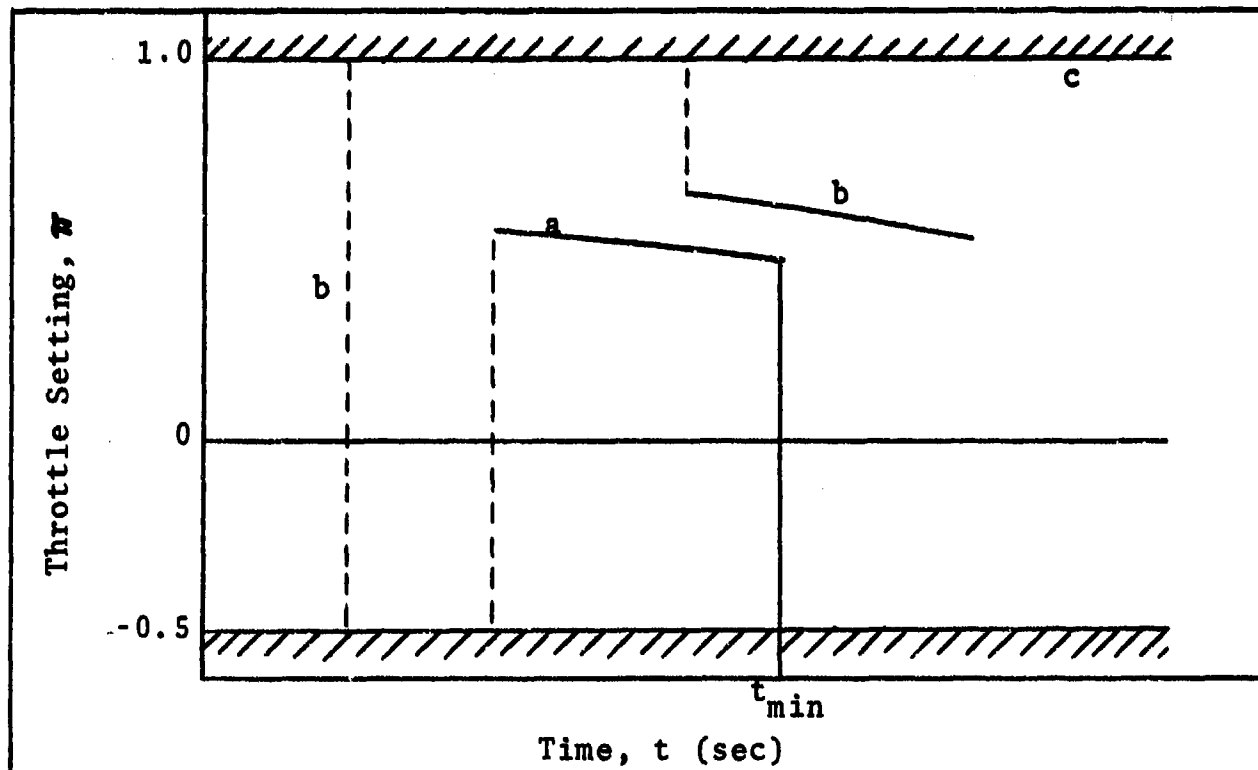
Figure 6-5. Throttle Setting vs. Time for $V_i > V_c$
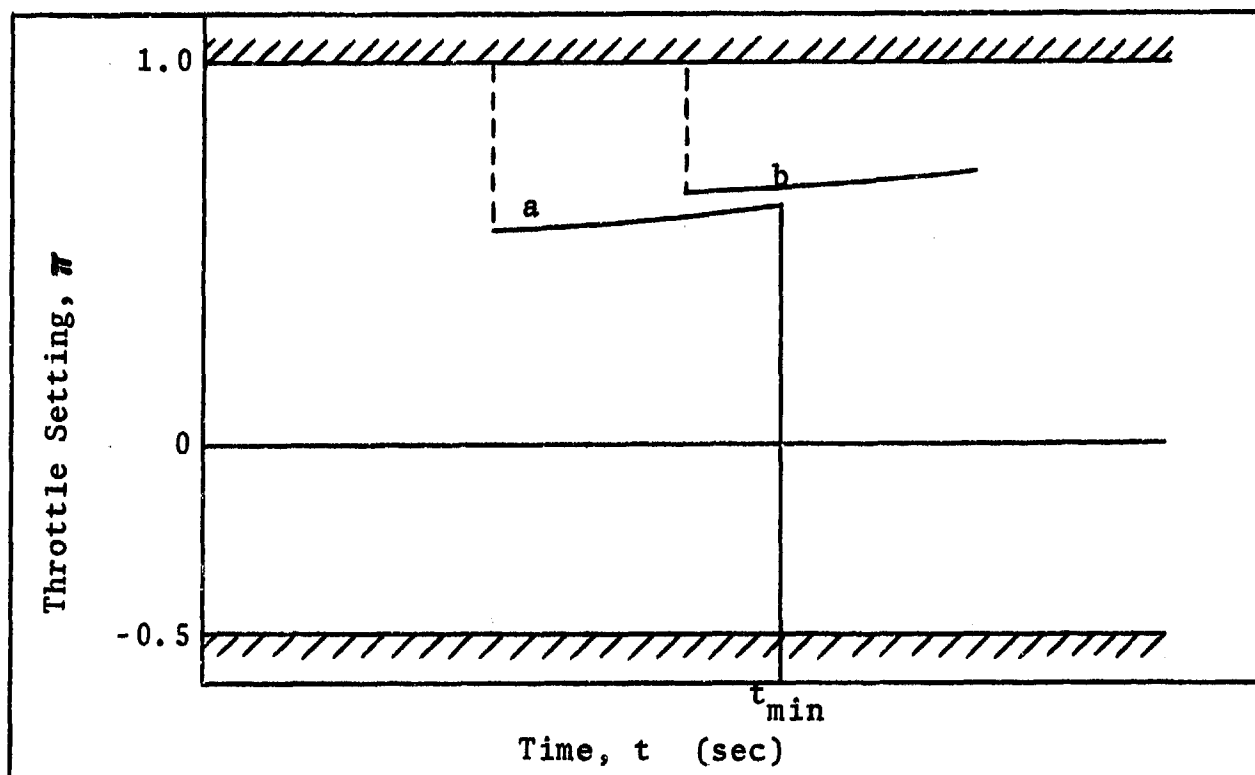
Figure 6-6. Throttle Setting vs. Time for $V_i < V_c$

VII. <u>RESULTS OBTAINED</u>

The equations, conditions and constraints for all three problem formulations, set forth in sections 4 and 5, were programmed on a 32 bit DEC 20/20 digital computer in the Space Division Computer Center. A copy of the computer programs, OPTMYZ and its subroutines, are located in the appendix. The results of this program's execution are presented in this section.

Minimum Time-to-Turn Results

As the costate variables determine the optimal controls which in turn, determine the state trajectories, the results are presented in that order. Time history plots for the costates, controls and states are presented in figures 7-1 through 7-9. By examining these plots, several observations can be made.

First, the costate histories figs (7-1) through (7-3) are well behaved and are primarily monotonic; the discontinuities in λ_h and λ_v do not create erratic behavior or unexpected characteristics. It may be coincidence and of no consequence but it is of interest to note that for λ_h when $t < tc$, is virtually a constant while C_L is on the N_{max} boundary for the high speed solution but varies smoothly when C_L is equal to $C_{L_{max}}$ for the low speed solution. Otherwise, λ_h acted as expected. λ_v responded per the optimal control requirements of Eq (4-24) through Eq (4-32). It

43

Figure 7-1. λ_h vs Time for Minimum Time High and Low Speed Solutions

Figure 7-2. λ_v vs Time for Minimum Time High and Low Speed Solutions
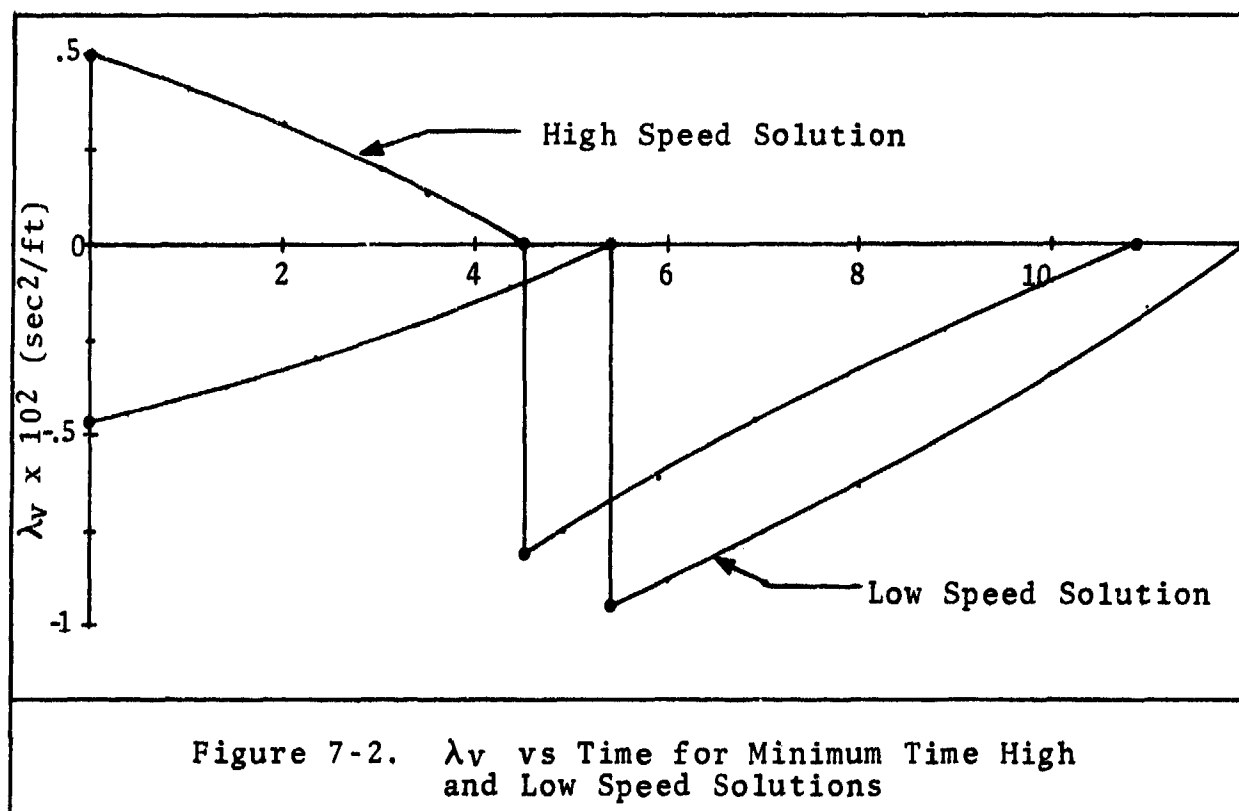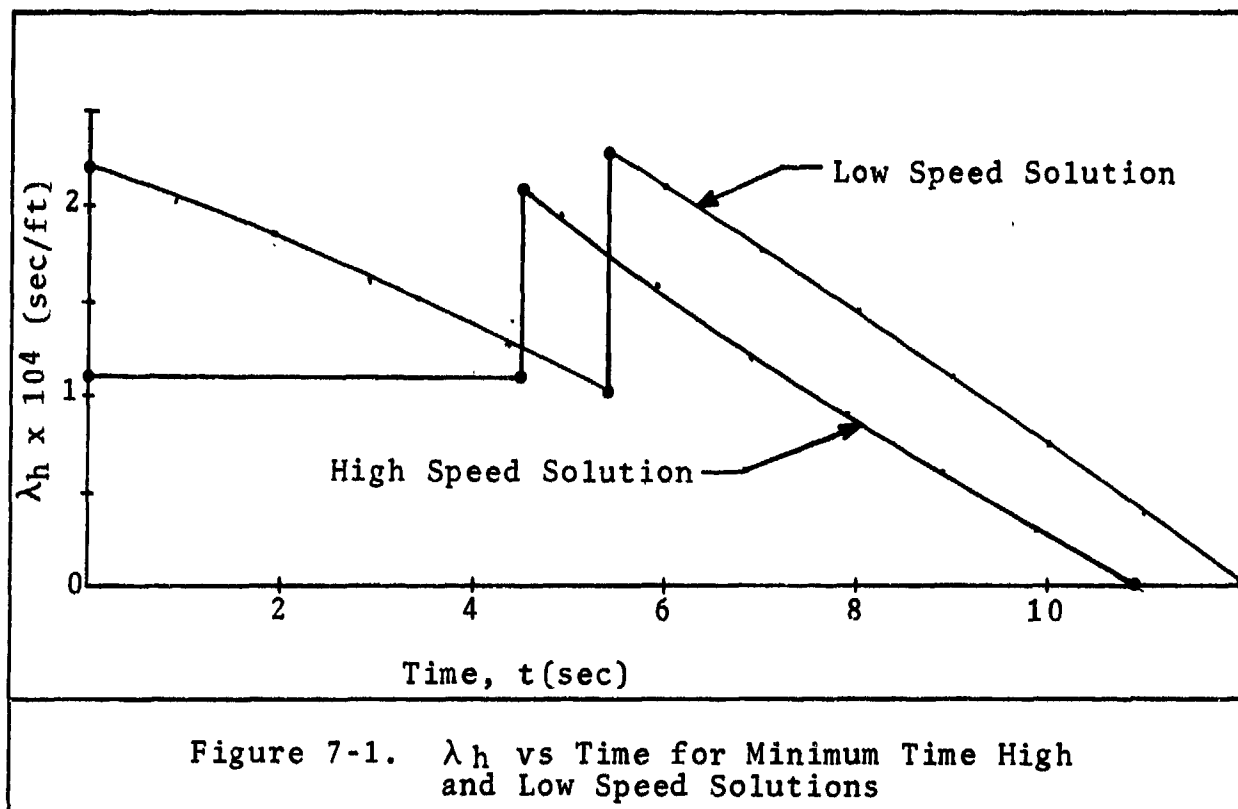
exhibited no unexpected trends. Figure 7-3 shows the correlation between the bank angle, flight path angle, λ_γ and the constant λ_ψ. The bank angle history can be determined from the plot using a protractor the same way as was done in fig (4-1) and can be correlated roughly to time using the tick marks at one second increments. Again, these parameters all vary smoothly with time.

The control histories are shown in figures (7-4) through (7-6). The bank angle history shapes were as expected although the amplitudes were larger than anticipated. The lift coefficient histories were exactly as expected for both high and low speed solutions. The shapes of the throttle histories were as expected, although like the bank angle, their excursions were greater than anticipated. As seen in fig (4-6), the singular arc portion of the solutions appear to go right up to the boundary denoted by the arrow heads. In actuality, the values of π at these two points are $\pi = 0.9999$ at $t = 6.12$ secs for the high speed solution and $\pi = -0.4997$ at $t = 6.22$ sec for the low speed solution thus keeping them interior to the boundaries. However, in order to insure that π remained interior, a special search routine in the integrator had to be programmed to look for the point, if one existed, where the arc touched the boundary, thus ending the arc. More will be said about this in the technique problems section. In retrospect, it makes sense that the throttle would go
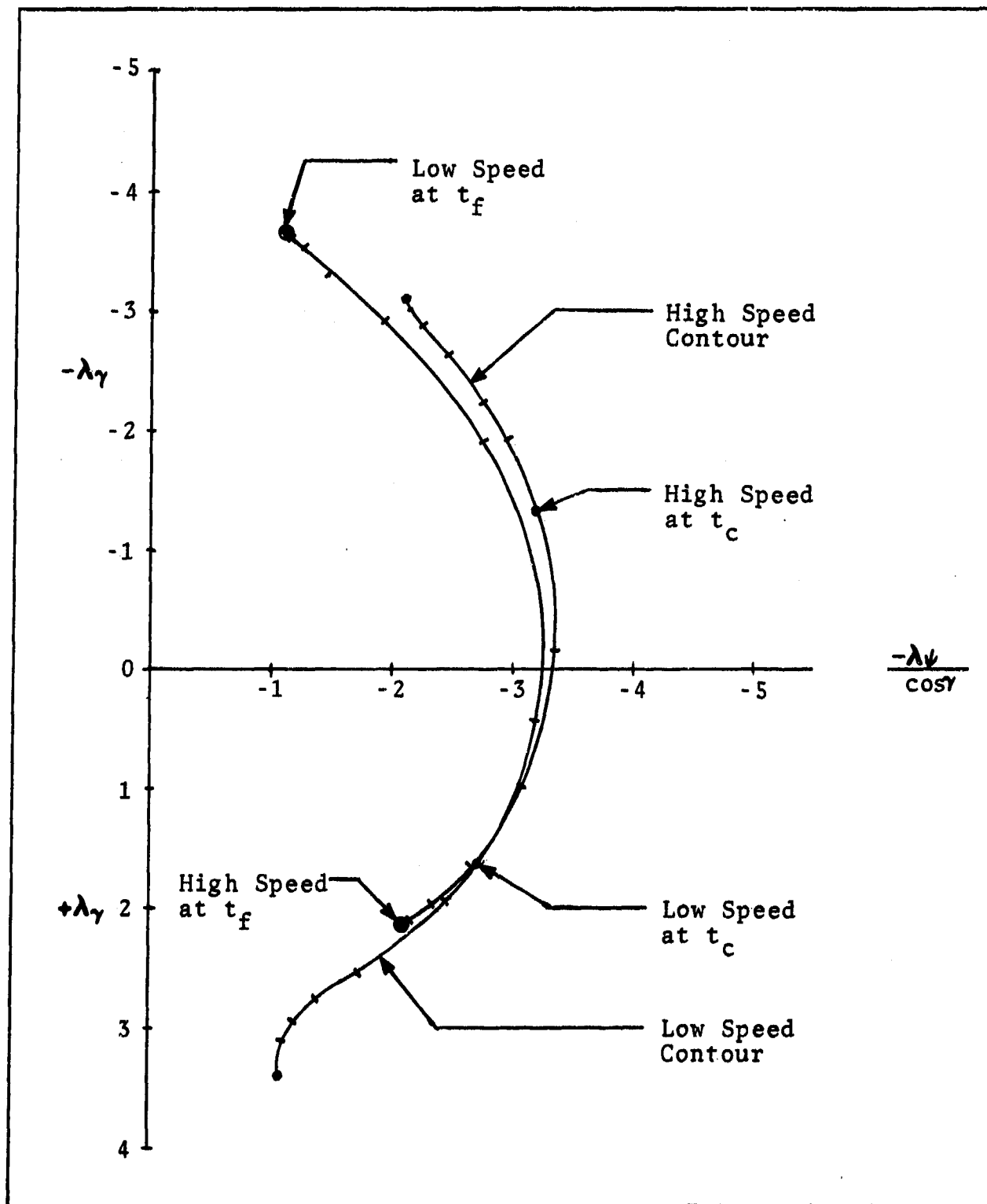
Figure 7-3. $-\lambda_\gamma$ vs $-\lambda_\psi/\cos\gamma$ Minimum Time Solutions.
Costate Migration Determining Bank Angle
History
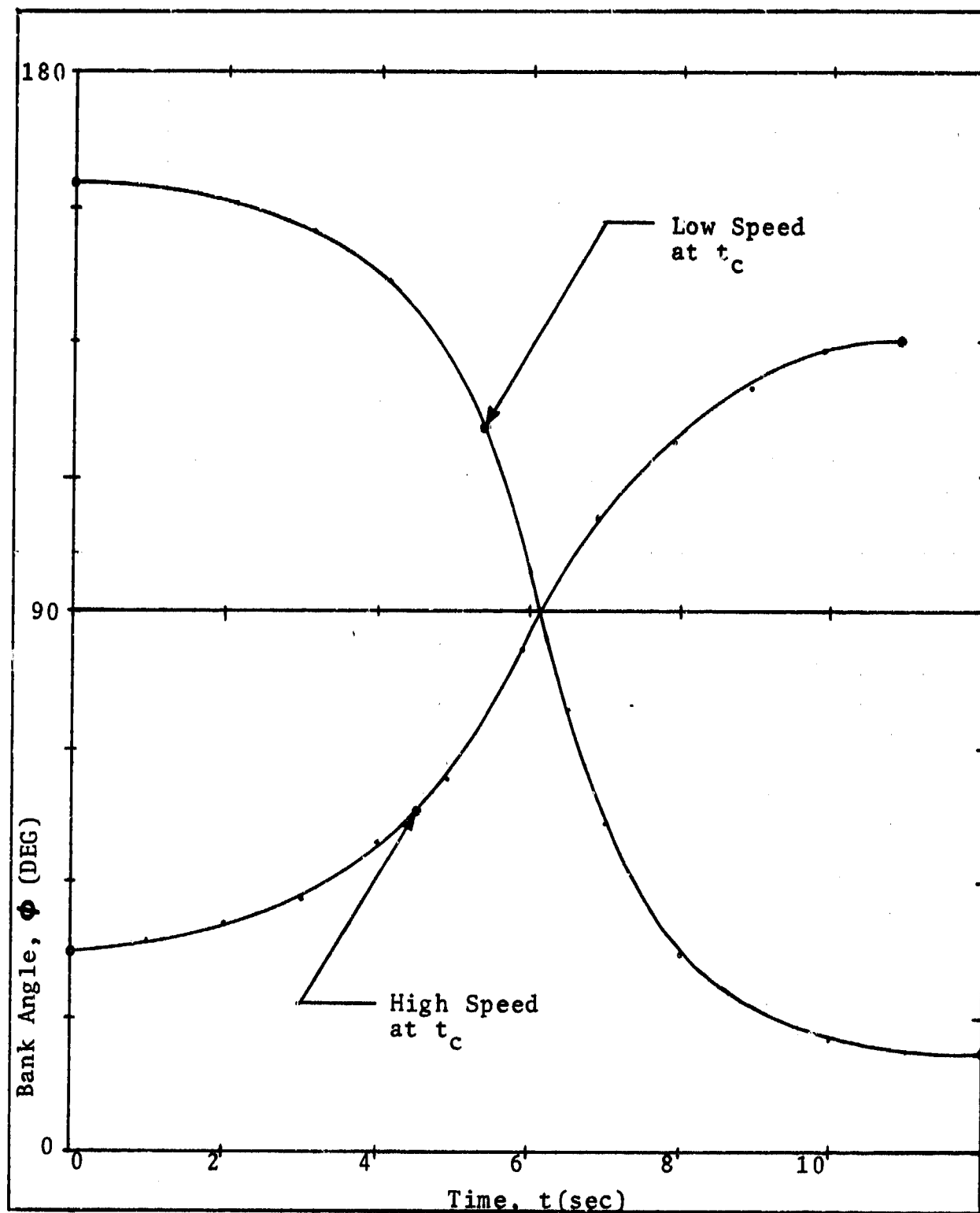
Figure 7-4.   Bank Angle vs Time for Minimum Time
High and Low Speed Solutions

Figure 7-5.   Lift Coefficient vs Time for Minimum Time
High and Low Speed Solutions

Figure 7-6.   Throttle Setting vs Time for Minimum Time
High and Low Speed Solutions
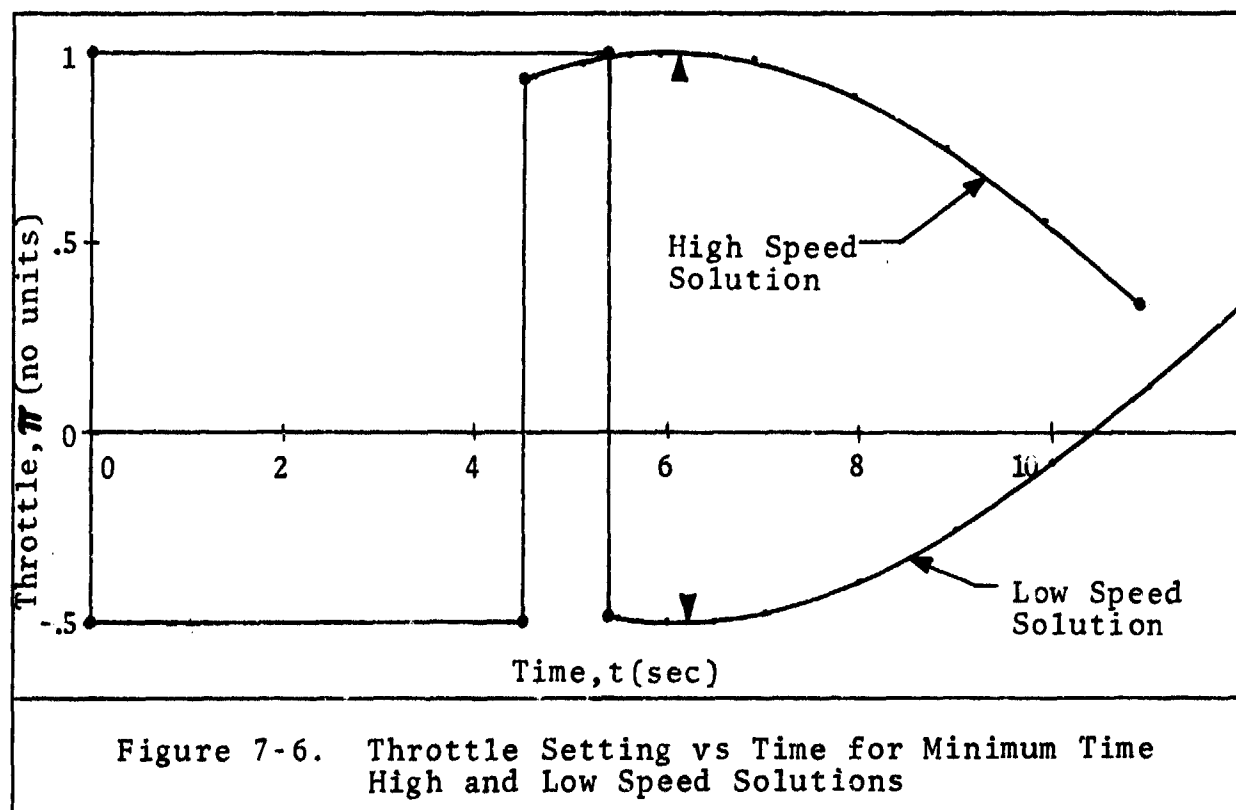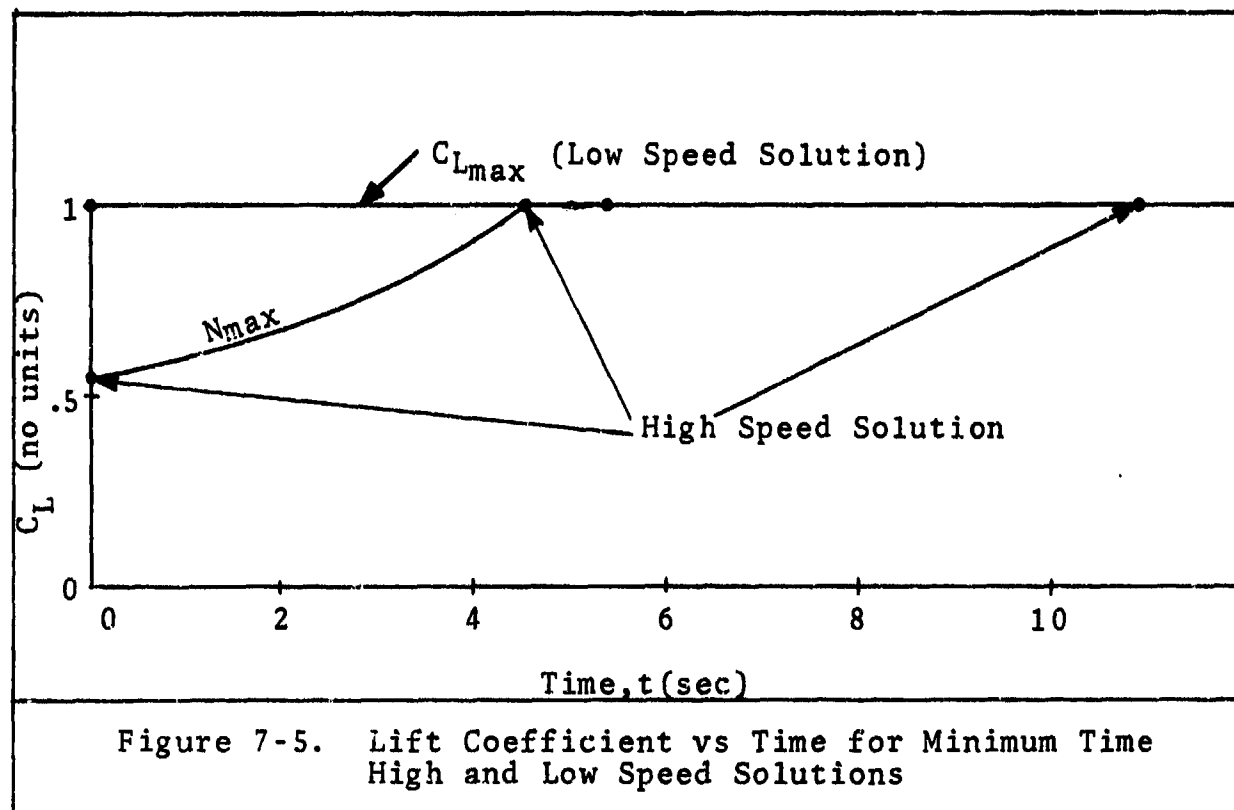
right up to the boundary even on the arc because the controls will use all of the authority they have to minimize the time to turn. Just as in a bang-bang controller, a bang-singular controller should be expected to go from boundary to boundary while meeting its interior control constraints.

Turning to the state trajectories starting with Fig (7-7) it is seen that both solutions end up on the singular arc and both met a small loss in energy (-262 ft for low speed and -1258 for high speed). Both maneuvers are basically planar, the steepness of which are dictated primarily by the initial bank angle values. This steepness correlates directly to the flight path angle histories of fig (7-8), the low speed being more vertical a maneuver than the high speed. The main reason for them not both being vertical plane maneuvers is that the throttle settings on the arc were already up against the boundary. However, increasing the thrust-to-weight ratio to approximately 1.9 or greater would result in two vertical maneuvers where the arc throttle histories would not be nearly so close to the boundaries because the use of gravity would be maximized. The heading angle histories show nothing unexpected. The low speed solution has higher peak turn rates due to the steeper flight path angle history. Tables (7-1) and (7-2) summarize the key values for the states and costates for the low and high speed solutions respectively. From both

Figure 7-7. Velocity and Down/Cross Range vs Energy Attitude for Minimum Time High and Low Speed Solutions
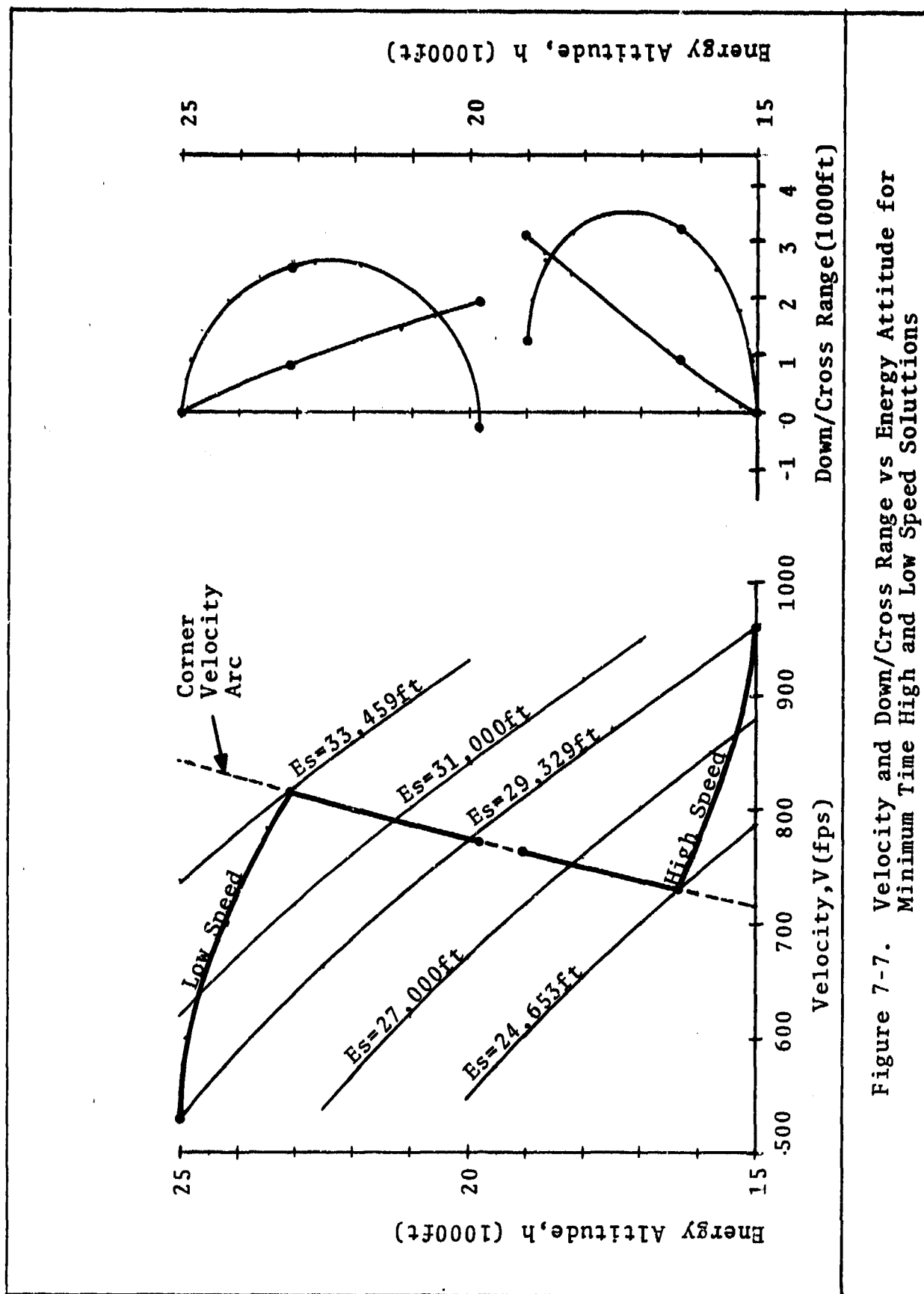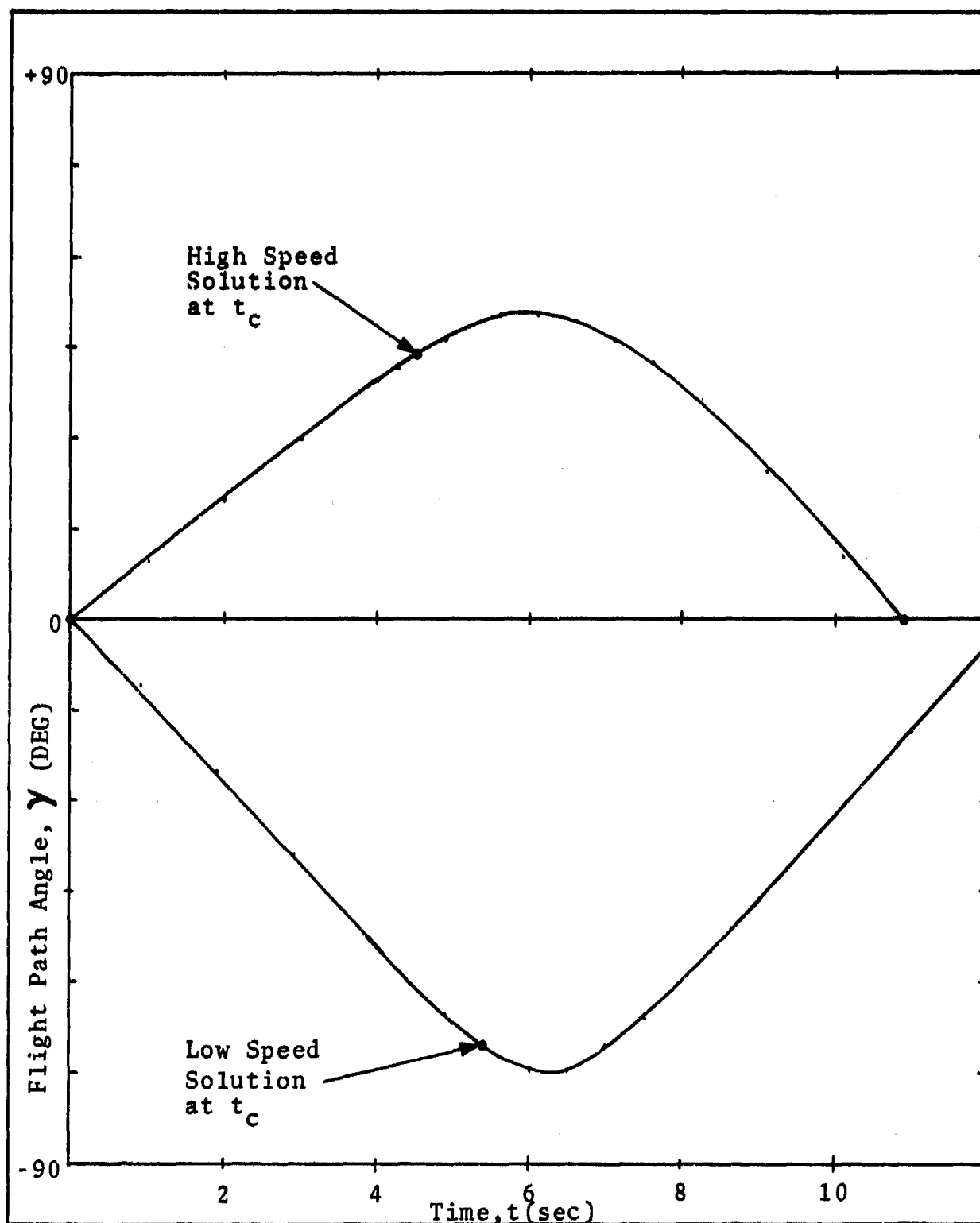
Figure 7-8. Flight Path Angle vs Time for Minimum
Time High and Low Speed Solutions
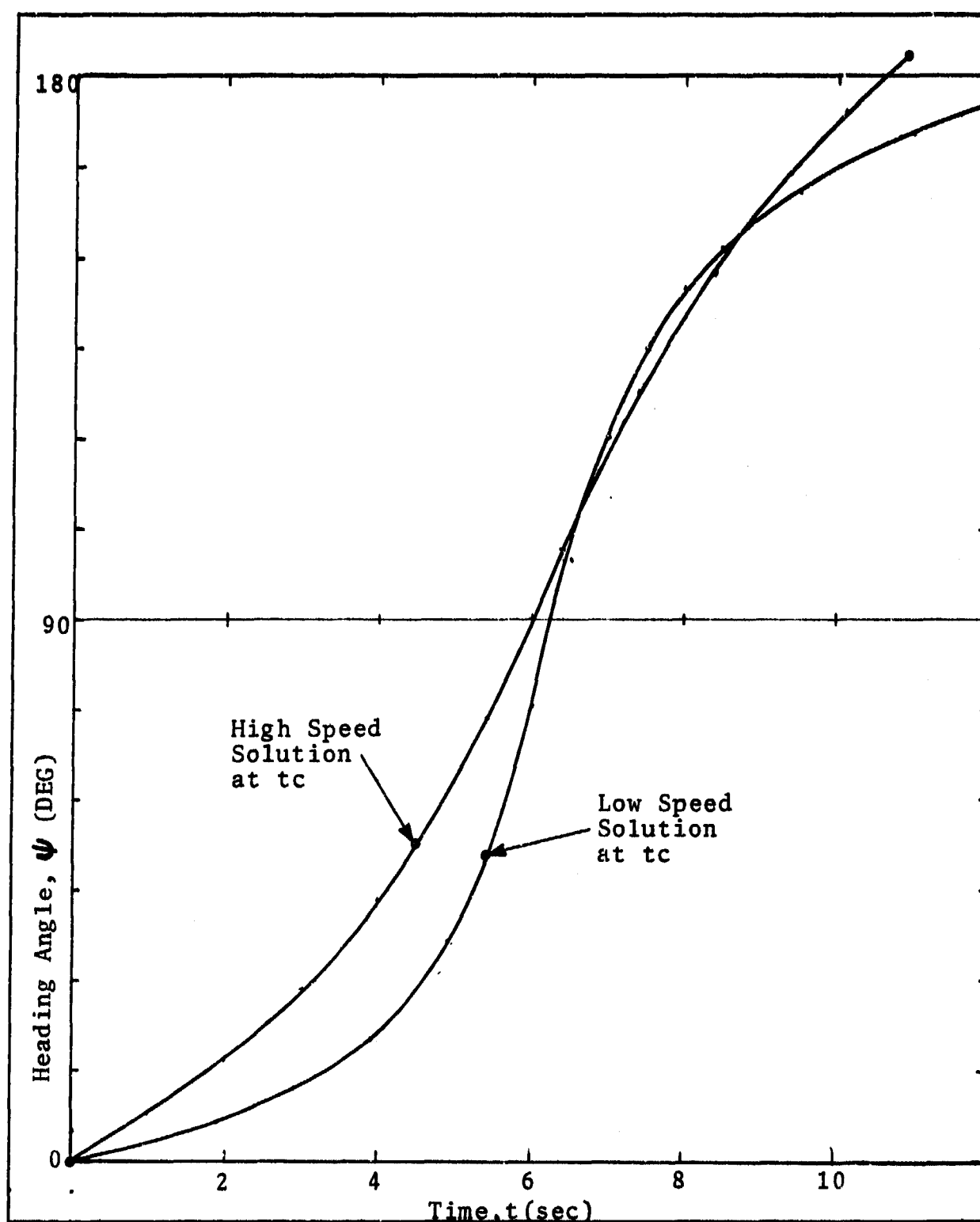
Figure 7-9.   Heading Angle vs Time for Minimum
Time High and Low Speed Solutions

	$t_f = 11.97$	$t_c^+ = 5.378 = t_c^-$		$t_o = 0$	R
λh	0	0.0002269	0.0001010	0.0002213	
λv	0	-0.009410	0	-0.004695	
λ_γ	-3.677	1.616		3.398	
λ_ψ	-1.087	-1.087		-1.087	
X	-285.6	2565.1		0	
Y	1981.9	818.0		0	
ΔE	-262	41.17		0	
h	19809	23123		24999.5	$r_h = -1.4626$
V	772.4	815.5		528.6	$r_v = 0.7539$
γ	0	-1.158		0.0787	$r_\gamma = 0.0787$
ψ	3.14159	0.9703		0.0782	$r_\psi = 0.0782$
					$\|R\| = 0.8914$

Table 7-1. End and Corner Values of States and Costates for Low Speed Minimum Time Solution

	$t_f = 10.87$	$t_c^+ = 4.495 = t_c^-$		$t_o = 0$	R
λh	0	0.0002078	0.0001103	0.0001101	
λv	0	-0.008138	0	0.005010	
λ_γ	2.120	-1.917		-3.108	
λ_ψ	-2.1075	-2.1075		-2.1075	
X	1239.5	3252.2		0	
Y	3082.0	965.6		0	
ΔE	-1251.8	-4668.3		0	
h	19033	16372		14998.3	$r_h = -1.7438$
V	762.6	730.0		960.05	$r_v = 0.3734$
γ	0	0.7714		0.006517	$r = 0.006517$
ψ	3.14159	0.8626		0.06289	$r = 0.06289$
					$\|R\| = 1.7555$

Table 7-2. End and Corner Values of states and costates for High Speed Minimum Time Solution

tables, it is seen that the end conditions were not met to the accuracy that was expected. The norms of the residual vectors shown are as low as could possibly be achieved with the program, computer and methodology employed.

Problems with the Technique

The search for the optimal controls began by using a variable stepsize integrator and allowing only small increases in the total time allotted for the turn to occur on each iteration to insure stability in approaching the solution. However, after achieving a norm of the residual vector of approximately 10, fixed stepsize integration had to be employed. The prime reason for this is due to the special programming which had to be added to the integrator to find the point in time where π went so close to or touched the boundary during the search phase. This search could not be performed using variable stepsize integration.

The use of small, fixed stepsize integration helped to get closer to the optimal solution, but the extreme sensitivity of the norm of the residual vector to the final value of λ_γ created havoc with finding the minimum in the state space. As shown in fig (7-10), it is seen that the standard parabolic minimum seen in bang-bang minimum time problems has been replaced with a gross discontinuity in the norm at the point where the
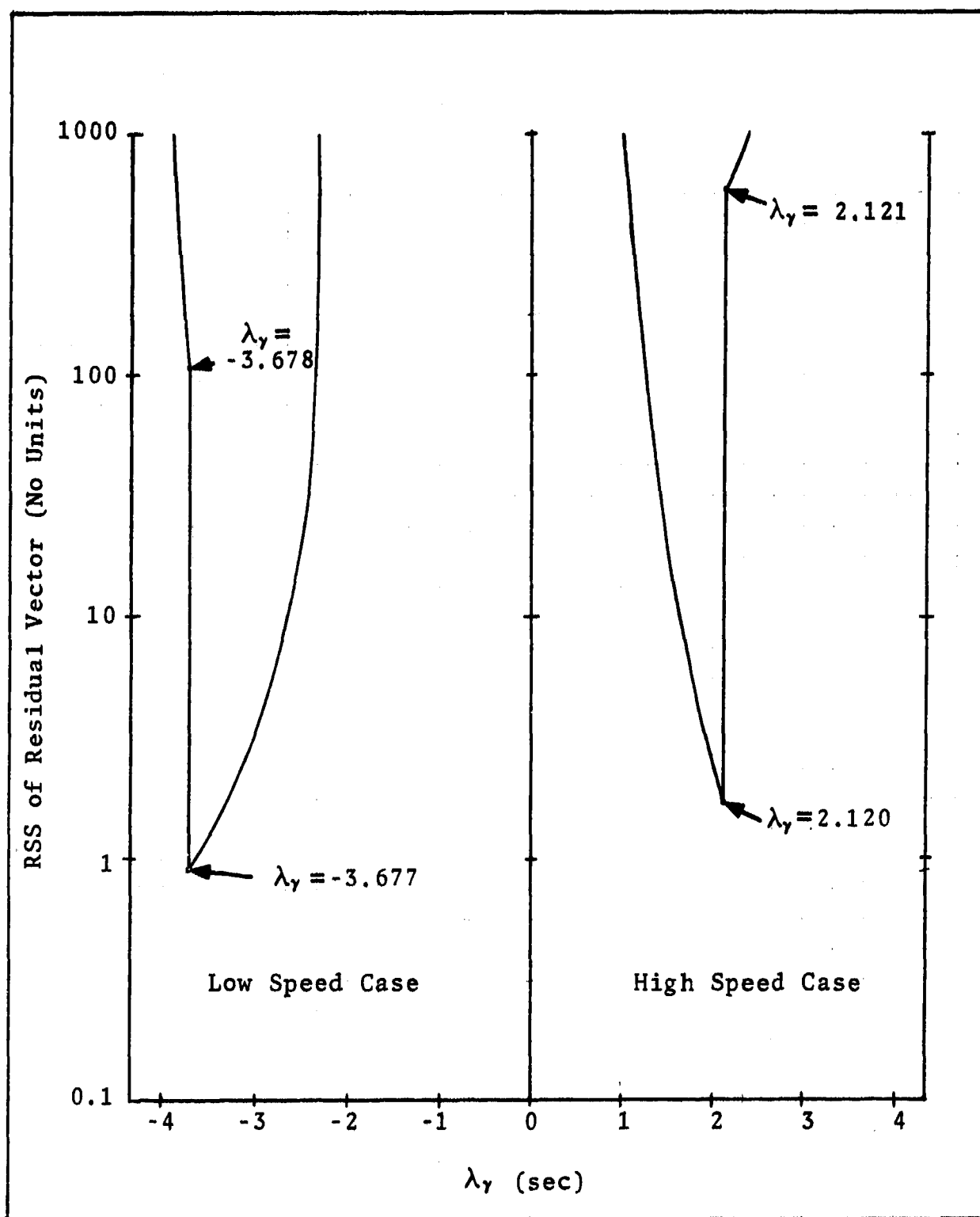
Figure 7-10.   Norm of Residual Vector vs λ_γ for
             Minimum Time High and Low Speed Solutions

magnitude of λ_y gets large enough to create a steeply banked planar maneuver which causes π to require a boundary value at the arrow head points on fig (7-6). This causes the time at which the switch from the singular arc to the boundary value control to snap back and forth during the search for the minimum. In the low speed case, the change in λ_y from -3.677 to -3.678 caused a discontinuous jump in the norm from less than 1.0 to more than 100. Whether the sensitivity matrix for calculating δz was formed using a forward, central or backward difference scheme was immaterial. The z components being so tightly coupled could not be modified so slightly in the proper δz direction to reduce the norm any further than that shown in tables (7-1) and (7-2).

Even though the end conditions were not met close enough to form a residual norm of 10^{-4} or less, the trajectories shown are extremely close to the optimum and demonstrate that the technique and problem formulation are correct and feasible.

Maximum Energy Turn Results

No feasible trajectories were generated for the maximum energy turn formulation which came close to the desired end conditions. No norm of the end conditions could be achieved which was less than 50 to 20 in magnitude. Innumerable attempts were made to find a

single set of final time conditions which would generate one feasible trajectory from which to propagate the others. Several fixed final times were used as starting points, but all times generated approximately the same end results. The multipliers λ_γ and λ_ψ grew an order of magnitude with each iteration surpassing values of 10^{13} and growing with no reasonable reduction in the end condition norm. No definite reason can be given for this type of performance; perhaps the linearity of the aircraft thrust and drag characteristics create a flat state space where there is no obvious maximum energy turn.

Since no maximum energy turn solutions were achieved, the graphical method of fig (2-1) for depicting the energy-time tradeoff can not be used.

Maximum Energy Gradient Results

Unfortunately, the same type of results, as in the maximum energy turn attempt, occurred here as well. The values for λ_γ and λ_ψ were in the vicinity of 10^8 and growing steadily showing no reduction in the norm of the end conditions. Additionally, the final time would not settle in one neighborhood but would grow and decrease as the attempts progressed. Once again, no positive explanation can be offered other than presented in the previous section.

No maximum energy gradient solution was achieved

using this method either. All three problems used pure optimal control formulations and ran into extreme difficulty in achieving a solution. Evidently, these formulations do not lend themselves well to methods using Lagrange multiplier techniques and may be more well suited for parameter optimization formulations.

VIII.   CONCLUSION

The goal of this effort was to define a tradeoff between time-to-turn and energy in a turn using the classical optimal control formulation.   First, a minimum time-to-turn trajectory was to be generated for initial conditions of equal energy both above and below the corner velocity for that energy.   Second, maximum energy trajectories beginning at those same initial conditions were to be generated for final times greater than the minimum time.   From all of these trajectories, the maximum energy gradients, defining the time-energy tradeoffs, were to be graphically identified.   Thirdly, these tradeoffs were to be corroborated using the maximum energy gradient formulation.

This project was successful in defining the equations, conditions and constraints required to reach the above goals. The computer program OPTMYZ was written and executed on a DEC 20/20 digital computer which was successful in defining the two minimum time trajectories for the initial conditions above and below the corner velocity conditions.   The results are presented in section 7.

This effort failed to produce feasible maximum energy turns or the maximum energy gradients required for the tradeoff definition. Therefore the time-energy trade can not be identified for either of the initial conditions

60

for the aircraft model used and the formulations employed.

Recommendations for further work in this area are presented in section 9.

IX. RECOMMENDATIONS

The following are prioritized recommendations for further research in the area of time-energy tradeoffs.

1) Continued effort should be placed upon defining the time-energy tradeoffs as defined in section 2 using the formulations presented herein. Emphasis should be placed upon developing a technique which will better determine the minimum cost function for a complex singular arc problem such as the minimum time problem presented.

2) The time-energy tradeoff should also be determined as in recommendation (1) using a parameter optimization formulation to study the tradeoff of complexity versus accuracy. Based upon these results, the remaining recommendations would use the superior technique for future work.

3) Recommendations (1) and (2) should then be repeated using a more realistic aircraft model. There should remain regions in the altitude velocity map where high specific power exists, but the thrust should vary as a function of altitude and Mach or Reynolds number as should the lift and drag parameters. $C_{L_{max}}$, C_{D_O} and k. A thrust

pinch, dynamic pressure, Mach number and altitude placards could be added for realism.

4) Recommendation (3) should be repeated with the addition of a fuel flow or varying weight and where

$$\dot{W} = -c|\pi| \tag{9-2}$$

5) Recommendation (4) should be repeated with the performance index modified to pay a penalty for excessive fuel consumption. That is

$$G\ x(t_f), t_f = -\left[\frac{h_f - h_i}{(W_f - W_i)t_f} + \frac{V_f^2 - V_i^2}{2g(W_f - W_i)t_f}\right] \tag{9-3}$$

This effort would be the most direct way of looking at trading time and fuel for energy with the most realistic model for an aircraft.

6) Using the results from the previous recommendations, a quasi-linear feedback law could be developed for two modes of operation. The first mode would be an algorithm for minimum time turn guidance free from the use of influence functions and the second mode would be for a maximum time-energy-fuel tradeoff based upon only state and state rate feedback.

7) The culmination of this series of efforts
would be to program these feedback laws into
a manned simulator with visuals and head-up
displays to examine the man-machine
applicability.

Bibliography

1. Anderson, Gerald M. and W.L. Othling Jr. "Optimal Trajectories of High Thrust Aircraft," _Journal of Aircraft_, 13: 180-184 (March 1976).

2. Bryson, A.E., W.F. Denham and S.E. Dreyfuss. "Optimal Programming Problems with Inequality Constraints," _AIAA Journal_, 1: 2544-2550 (Nov 1963).

3. Bryson, A.E. and Y.C. Ho. _Applied Optimal Control_ (Second Edition). Washington, D.C.: Hemisphere Publishing Company, 1975.

4. Hedrick, J.K. and A.E. Bryson. "Three Dimensional Minimum Time Turns for a Supersonic Aircraft," _Journal of Aircraft_, 9: 115-121 (February 1972).

5. Humphreys, Robert P., G.R. Hennig, W.A. Bolding and L.A. Helgeson. "Optimal Three Dimensional Minimum Time Turns for an Aircraft," _Journal of Astronautical Sciences_, 20: 88-112 (September-October 1972).

6. Ketter, R.L. and S.P. Prawel Jr. _Modern Methods of Engineering Computation_. New York: McGraw-Hill Book Company, 1969.

7. Miele, Angelo A. "Recent Advances in Gradient Algorithms for Optimal Control Problems," _Journal of Optimization Theory and Applications_, 17: 361-430 (December 1975).

8. National Oceanic and Atmospheric Administration. _U.S. Standard Atmosphere, 1976_. Washington, D.C.: National Aeronautics and Space Administration, United States Air Force, 1976.

9. Newman, William M. and R.F. Sproul. _Principals of Interactive Computer Graphics_. New York: McGraw-Hill Book Company, 1973.

10. Nicolai, Leland M. _Fundamentals of Aircraft Design_. Fairborn: E.P. Domicone Printing Services, 1975.

11. Noble, Ben and J.W. Daniel. _Applied Linear Algebra_. Engelwood Cliffs: Prentice-Hall, Incorporated, 1977.

12. Rader, James E. Lecture Notes distributed during the Optimization Techniques Sequence. School of Engineering, Air Force Institute of Technology, Wright-Patterson AFB, 1978.

13. Rader, James E. and D.G. Hull. "Computation of Optimal Aircraft Trajectories using Parameter Optimization Methods," _Journal of Aircraft, 12:_ 864-866 (November 1975).

14. Wylie, C.R. _Advanced Engineering Mathematics._ New York: McGraw-Hill Book Company, 1966.

15. Yajnik, K.S. "Energy-Turn Rate Characteristics and Turn Performance of an Aircraft," _Journal of Aircraft, 14:_ 428-432 (May 1977).

Appendix

Computer Program:

OPTMYZ

```
      program optmyz
      dimension x(10),xf(10),xi(10),dx(4),r(4),rm(4),rp(4),dz(4),
     &drdz(4,4),drdzi(4,4),d(4,4)
      real k,nmax
      common a,beta,clmax,cdo,g,k,nmax,tmax,w,xi4
      common clnmax,hfifi,jflag,qa,rosig
      data xi(6),xi(7),xf(6),xf(7)/0.0,0.0,0.0,3.14159/
      data a,beta,clmax,cdo,g,k,nmax,tmax,w/
     &237.0,-0.000032811628,1.0,0.02,32.174,0.05,7.22,
     &18225.0,12150.0/
      write(5,1)
    1 format(1x,'load lflag for tmin,Emax or Edotmax')
      read(5,*) lflag
      write(5,2)
    2 format(1x,'load hf,lambdagammaf,lambdapsif,tf,tc,hi,vi')
      read(5,*) xf(1),xf(2),xf(3),tf,tc,xi(1),xi(4)
      xi4=xi(4)
      write(5,3)
    3 format(1x,'do you wish to print each step(yes=0,no=1)?')
      read(5,*) iprint
      call assign(xf,xi,tf,lflag)
      do 4 i=1,10
    4 x(i)=xf(i)
      call integ(10,x,tf,tc,iprint)
      xf(9)=-x(9)
      xf(10)=-x(10)
      call ndmiss(x,xi,r,rnorm)
      write(5,5) r,rnorm
    5 format(1x,'r and rnorm',/,5(1x,f10.4))
      it=0
    6 it=it+1
      write(5,7)
    7 format(1x,'do you want to continue?')
      read(5,*) choice

      if(choice.eq.0) go to 16
      if(rnorm.le.1.0000) go to 16
      do 12 i=1,4
      ii=i
      iii=1
      do 8 j=1,10
    8 x(j)=xf(j)
      tfs=tf
      tcs=tc
      write(5,81)
   81 format(1x,'deltas')
      call deltas(x,dx,tfs,tcs,lflag,ii,iii)
      write(5,81)

      write(5,82)
   82 format(1x,'assign')
      call assign(x,xi,tfs,lflag)
      write(5,82)
      write(5,83)
   83 format(1x,'integ')
```

```
      call integ(10,x,tfs,tcs,iprint)
      write(5,83)
      write(5,84)
   84 format(1x,'ndmiss')
      call ndmiss(x,xi,rp,rnormp)
      write(5,84)
      write(5,9) rp,rnormp
    9 format(1x,'rp and rnormp',/,5(1x,f10.4))
      iii=01
      do 10 j=1,10
   10 x(j)=xf(j)
      tfs=tf
      tcs=tc
      call deltas(x,dx,tfs,tcs,lflag,ii,iii)
      call assign(x,xi,tfs,lflag)
      call integ(10,x,tfs,tcs,iprint)
      call ndmiss(x,xi,rm,rnormm)
      write(5,11) rm,rnormm
   11 format(1x,'rm and rnormm',/,5(1x,f10.4))
      do 12 j=1,4
   12 drdz(j,i)=(rp(j)#rm(j))/(2.0*dx(i))
      write(5,13) dx
   13 format(1x,'dx',/,4(1x,f14.7),/)
      call mtxinv(drdz,drdzi,d,4)
      do 14 i=1,4
      dz(i)=0.0
      do 14 j=1,4
   14 dz(i)=dz(i)#drdzi(i,j)*r(j)
      write(5,15) dz
   15 format(1x,'dz',/,4(1x,f10.4),/)
      call search(xf,xi,tf,tc,dz,r,rnorm,lflag,iprint)
      write(5,17) xf,tf,tc,r,rnorm
      if(rnorm.gt.1.0000) go to 6
   16 write(5,17) xf,tf,tc,r,rnorm
   17 format(1x,'xf,tf,tc,r,rnorm',/,2(5(1x,f13.7),/),
     &2(1x,f10.6),/,5(1x,f13.7))
      if(choice.eq.0) go to 20
      do 18 i=1,10
   18 x(i)=xf(i)
      call integ(10,x,tf,tc,0)
      call ndmiss(x,xi,r,rnorm)
      write(5,19) x,tf,tc,r,rnorm

   19 format(1x,'x,tf,tc,r,rnorm',/,2(5(1x,f13.7),/),
     &2(1x,f10.6),/,5(1x,f13.7))
   20 stop
      end
```

```
      subroutine assign(x,xi,tf,lflag)
      dimension x(10),xi(10)
      real nmax
      data beta,g,nmax/-0.000032811628,32.174,7.22/
      x(4)=558.07441*sqrt(exp(-beta*x(1)))
      if(lflag.eq.2) go to 10
      Ei=xi(1)+xi(4)**2/2.0/g
      E=x(1)+x(4)**2/2.0/g
      if(lflag.eq.1) Gtf=1.0
      if(lflag.eq.3) Gtf=(E-Ei)/tf**2
      x2min=-Gtf*x(4)/200.123
      x2max=Gtf*x(4)/264.471
      if(x(2).lt.x2min) x(2)=x2min
      if(x(2).gt.x2max) x(2)=x2max
      x(3)=-sqrt((x(4)/g/nmax)**2*(Gtf-x(2)*g/x(4))**2-x(2)**2)
      x(5)=0.0
      x(8)=0.0
      if(lflag.eq.1) go to 20

 10   x(5)=-1.0
      x(8)=-x(4)/g
      if(lflag.eq.2) go to 20
      x(5)=x(5)/tf
      x(8)=x(8)/tf
 20   return
      end
```

```
subroutine integ(n,x,tf,tc,iprint)
dimension x(10)
real k,nmax
common a,beta,clmax,cdo,g,k,nmax,tmax,w,xi4
common clnmax,hfifi,jflag,qa,rosig
jflag=0
dt=00.25
tcs=tc
call rk78(n,x,tf,tcs,dt,tc,iprint)
x(5)=x(5)+x(8)*beta*x(4)/2.0
x(8)=0.0
tcx=tcs+1.0e+06
dt=00.25
call rk78(n,x,tcx,0.0,dt,tcs,iprint)
tc=tcs
return
end
```

```
      subroutine rk78(n,x,t1,t2,dt,tc,iprint)
      dimension alph(13),b(13,12),ch(13),x(10),xdum(10)
      dimension f1(10),f2(10),f3(10),f4(10),f5(10),f6(10),f7(10),
     &f8(10),f9(10),f10(10),f11(10),f12(10),f13(10)
      real k,nmax,mu2,mu3
      common a,beta,clmax,cdo,g,k,nmax,tmax,w,xi4
      common clnmax,hfifi,jflag,qa,rosig
      data (alph(i),i=1,13)/
     &0.                      ,0.740740740740740e-01,0.1111111111111111e+00,
     &0.1666666666666666e+00,0.4166666666666666e+00,0.5          e+00,
     &0.8333333333333333e+00,0.1666666666666666e+00,0.6666666666666666e+00,
     &0.3333333333333333e+00,1.0          e+00,0.        ,
     &1.0          e+00/
      data ((b(i,j),i=1,13),j=1,3)/

     &0.                      ,0.740740740740740e-01,0.277777777777777e-01,
     &0.4166666666666666e-01,0.4166666666666666e+00,0.5          e-01,
     &0.2314814814814814e+00,0.1033333333333333e+00,2.0          e+00,
     &0.8425925925925925e+00,0.5812195121951210e+00,0.1463414634146341e-01,
     &0.4334146341463410e+00,0.                      ,0.                      ,
     &0.8333333333333333e-01,0.                      ,0.                      ,
     &0.                      ,0.                      ,0.                      ,
     &0.                      ,0.                      ,0.                      ,
     &0.                      ,0.                      ,0.                      ,
     &0.                      ,0.                      ,0.125        e+00,
     &0.15625          e+01,0.                      ,0.                      ,
     &0.                      ,0.                      ,0.                      ,
     &0.                      ,0.                      ,0.                      /
      data ((b(i,j),i=1,13),j=4,6)/
     &0.                      ,0.                      ,0.                      ,
     &0.                      ,0.15625          e+01,0.25          e+00,
     &0.1157407407407407e+01,0.                      ,0.8833333333333333e+01,
     &0.2129629629629630e+00,0.2079268829268293e+01,0.                      ,
     &0.2079268829268293e+01,0.                      ,0.                      ,
     &0.                      ,0.                      ,0.                      ,
     &0.2          e+00,0.2407407407407741e+01,0.2711111111111111e+00,
     &0.1564444444444444e+02,0.7229629629629630e+01,0.4386341463414630e+01,
     &0.                      ,0.4386341463414630e+01,0.                      ,
     &0.                      ,0.                      ,0.                      ,
     &0.                      ,0.                      ,0.2314814814814810e+01,
     &0.2222222222222222e+00,0.1188888888888880e+02,0.5759259259259260e+01,
     &0.3670731707317070e+01,0.1463414634146340e+00,0.3524390243902440e+01/
      data ((b(i,j),i=1,13),j=7,9)/
     &0.                      ,0.                      ,0.                      ,
     &0.                      ,0.                      ,0.                      ,
     &0.                      ,0.1444444444444444e-01,0.7444444444444444e+00,
     &0.3166666666666666e+00,0.5202439024390240e+00,0.1463414634146340e-01,
     &0.5348780487804880e+00,0.                      ,0.                      ,
     &0.                      ,0.                      ,0.                      ,
     &0.                      ,0.                      ,0.                      ,
     &0.3          e+01,0.2833333333333333e+01,0.5487804878048780e+00,
     &0.7317073170731710e-01,0.6219512195121950e+00,0.                      ,
     &0.                      ,0.                      ,0.                      ,
     &0.                      ,0.                      ,0.                      ,
     &0.                      ,0.                      ,0.8333333333333333e-01,
```

```
     &0.274390243902439e+00,0.731707317073170e+01,0.201219512195122e+00/
      data ((b(i,j),i=1,13),j=10,12)/
     &0.                     ,0.                     ,0.                     ,
     &0.                     ,0.                     ,0.                     ,
     &0.                     ,0.                     ,0.                     ,
     &0.                     ,0.439024390243902e+00,0.146341463414634e+00,
     &0.292682926829268e+00,0.                     ,0.                     ,
     &0.                     ,0.                     ,0.                     ,
     &0.                     ,0.                     ,0.                     ,
     &0.                     ,0.                     ,0.                     ,
     &0.                     ,0.                     ,0.                     ,
     &0.                     ,0.                     ,0.                     ,
     &0.                     ,0.                     ,0.                     ,
     &0.                     ,0.                     ,0.                     ,
     &0.                     ,0.                     ,1.0            e+00/
      data (ch(i),i=1,13)/
     &0.                     ,0.                     ,0.                     ,
     &0.                     ,0.                     ,0.323809523809524e+00,
     &0.257142857142857e+00,0.257142857142857e+00,0.321428571422857e+01,
     &0.321428571428571e+01,0.                     ,0.488095238095238e+01,
     &0.488095238095238e+01/
      data erps,tol,tolt/1.0e+06,1.0e+03,1.0e+04/
      t=t1
10    do 20 i=1,n
20    xdum(i)=x(i)

      if(iprint.eq.0) call printr(x,t,tc)
      call deriv(x,t,tc,f1)
      if(iprint.eq.0) call hamilt(t,x,f1,h)
      if(t.eq.t2.or.dt.eq.0.0) go to 250
30    continue
      b21=b(2,1)*dt
      do 42 i=1,n
42    x(i)=b21*f1(i)+xdum(i)
      call deriv(x,t,tc,f2)
      b31=b(3,1)*dt
      b32=b(3,2)*dt
      do 43 i=1,n
43    x(i)=b31*f1(i)+b32*f2(i)+xdum(i)
      call deriv(x,t,tc,f3)
      b41=b(4,1)*dt
      b43=b(4,3)*dt
      do 44 i=1,n
44    x(i)=b41*f1(i)+b43*f3(i)+xdum(i)
      call deriv(x,t,tc,f4)
      b51=b(5,1)*dt
      b53=b(5,3)*dt
      do 45 i=1,n
45    x(i)=b51*f1(i)+b53*(f3(i)+f4(i))+xdum(i)
      call deriv(x,t,tc,f5)
      b61=b(6,1)*dt
      b64=b(6,4)*dt
      b65=b(6,5)*dt
      do 46 i=1,n
46    x(i)=b61*f1(i)+b64*f4(i)+b65*f5(i)+xdum(i)
```

```
      call deriv(x,t,tc,f6)
      b71=b(7,1)*dt
      b74=b(7,4)*dt
      b75=b(7,5)*dt
      b76=b(7,6)*dt
      do 47 i=1,n
47 x(i)=b71*f1(i)+b74*f4(i)+b75*f5(i)+b76*f6(i)+xdum(i)
      call deriv(x,t,tc,f7)
      b81=b(8,1)*dt
      b85=b(8,5)*dt
      b86=b(8,6)*dt
      b87=b(8,7)*dt
      do 48 i=1,n
48 x(i)=b87*f7(i)+b81*f1(i)+b86*f6(i)+b85*f5(i)+xdum(i)
      call deriv(x,t,tc,f8)
      b91=b(9,1)*dt
      b94=b(9,4)*dt
      b95=b(9,5)*dt
      b96=b(9,6)*dt
      b97=b(9,7)*dt
      b98=b(9,8)*dt
      do 49 i=1,n
49 x(i)=b97*f7(i)+b91*f1(i)+b98*f8(i)+b94*f4(i)+b96*f6(i)+
     &b95*f5(i)+xdum(i)
      call deriv(x,t,tc,f9)
      b101=b(10,1)*dt
      b104=b(10,4)*dt
      b105=b(10,5)*dt
      b106=b(10,6)*dt
      b107=b(10,7)*dt
      b108=b(10,8)*dt
      do 50 i=1,n
50 x(i)=b32*f9(i)+b104*f4(i)+b107*f7(i)+b101*f1(i)+b108*f8(i)+
     &b106*f6(i)+b105*f5(i)+xdum(i)
      call deriv(x,t,tc,f10)
      b111=b(11,1)*dt

      b114=b(11,4)*dt
      b115=b(11,5)*dt
      b116=b(11,6)*dt
      b117=b(11,7)*dt
      b118=b(11,8)*dt
      b119=b(11,9)*dt
      b1110=b(11,10)*dt
      do 51 i=1,n
      f4(i)=b114*f4(i)+b115*f5(i)
51 x(i)=b119*f9(i)+b1110*f10(i)+b117*f7(i)+b118*f8(i)+
     &b111*f1(i)+f4(i)+b116*f6(i)+xdum(i)
      call deriv(x,t,tc,f11)
      b121=b(12,1)*dt
      b126=b(12,6)*dt
      b128=b(12,8)*dt
      do 52 i=1,n
52 x(i)=b121*(f1(i)+f7(i))+b128*(f8(i)+f9(i))+
     &b126*(f6(i)+f10(i))+xdum(i)
```

```
      call deriv(x,t,tc,f12)
      b131=b(13,1)*dt
      b136=b(13,6)*dt
      b137=b(13,7)*dt
      b138=b(13,8)*dt
      b139=b(13,9)*dt
      b1310=b(13,10)*dt
      do 53 i=1,n
   53 x(i)=b139*f9(i)+b1310*f10(i)+b131*f1(i)+b137*f7(i)+
     &b138*f8(i)+f12(i)*dt+f4(i)+b136*f6(i)+xdum(i)
      call deriv(x,t,tc,f13)
      c6=ch(6)*dt
      c7=ch(7)*dt
      c9=ch(9)*dt
      c12=ch(12)*dt
      do 100 i=1,n
  100 x(i)=xdum(i)+(c6*f6(i)+c7*(f7(i)+f8(i))+c9*(f9(i)+f13(i))+
     &c12*(f12(i)+f13(i)))
      dt1=dt
      if(t.lt.tc) go to 110
      call contrl(x,t,tc,mu2,mu3,phi,cl,pi)
      if(pi.ge.1.0.or.pi.le.00.5) jflag=1
      if(jflag.eq.1.and.pi.ge.1.0.or.pi.le.00.5) dt=dt1*0.98
      if(dt.eq.(0.98*dt1)) go to 30
      if(jflag.eq.1.and.pi.le.1.0.and.pi.ge.00.5) t2=t+dt1
  110 go to 200
      er=0.0
      do 150 j=1,n
      if(abs(x(j)).lt.erps) go to 150
      es=abs((f1(j)+f11(j)*f12(j)*f13(j))/x(j))
      if(es.gt.er)er=es
  150 continue
      er=er*abs(c12)+1.0e020
      dt=tolt/er
      dt=dt1*dt**0.125
      if(er.gt.tol) go to 30
      if(abs(dt).gt.0.25) dt=00.25
  200 t=t+dt1
      if(abs(dt).gt.abs(t2-t)) dt=t2-t
      go to 10
  250 return
      end
```

```
      subroutine printr(x,t,tc)
      dimension x(10)
      call contrl(x,t,tc,mu2,mu3,phi,cl,pi)
      fpa=x(6)*57.29577951
      psi=x(7)*57.29577951
      bank=phi*57.29577951
      write(5,10) t,(x(i),i=1,5),fpa,psi,(x(i),i=8,10),bank,cl,pi
   10 format(1x,f7.4,/,2(5(1x,e14.7),/),3(1x,f14.7),2(1x,e14.7))
      return
      end
```

```
      subroutine hamilt(t,x,f,h)
      dimension x(10),f(10)
      h=x(5)*f(1)+x(8)*f(4)+x(2)*f(6)+x(3)*f(7)
      write(5,1) x(5),f(1),x(8),f(4),x(2),f(6),x(3),f(7),h
    1 format(1x,'hamiltonian',3x,4(1x,e14.7),/,5(1x,e14.7))
      E=x(1)+x(4)**2/2.0/32.174
      write(5,2) E
    2 format(1x,'specific energy = ',e14.7)
      return
      end
```

```fortran
      subroutine deriv(x,t,tc,f)
      dimension x(10),f(10)
      real k,l,lh,mu2,mu3,nmax
      common a,beta,clmax,cdo,g,k,nmax,tmax,w,xi4

      common clnmax,hfifi,jflag,qa,rosig
      call contrl(x,t,tc,mu2,mu3,phi,cl,pi)
      l=qa*cl
      lh=l*beta
      d=qa*(cdo+k*cl**2)
      dh=d*beta
      cosg=cos(x(6))
      sing=sin(x(6))
      coss=cos(x(7))
      sins=sin(x(7))
      f(1)=x(4)*sing
      f(7)=g/x(4)/cosg*l/w*sin(phi)
      f(2)=cosg*(g*(x(8)+mu3*(1.0*beta*x(4)**2/2.0/g))*x(5)*x(4))
     &*sing*x(2)*g/x(4)*x(3)*f(7)*tan(x(6))
      f(3)=0.0
      f(4)=g*((tmax*pi*d)/w*sing)
      f(5)=g/w*(dh*(x(8)+mu3)+lh*(hfifi/x(4)*mu2))
      f(6)=g/x(4)*(l/w*cos(phi)*cosg)
      f(8)=2.0*f(5)/x(4)/beta+(x(2)*f(6)+x(3)*f(7))/x(4)
     &*sing*(x(5)+mu3*beta*x(4))
      f(9)=x(4)*cosg*coss
      f(10)=x(4)*cosg*sins
      return
      end
```

```
      subroutine contrl(x,t,tc,mu2,mu3,phi,cl,pi)
      dimension x(10)
      real k,l,nmax,mu2,mu3
      common a,beta,clmax,cdo,g,k,nmax,tmax,w,xi4
      common clnmax,hfifi,jflag,qa,rosig
      hfifi=sqrt(x(2)**2+(x(3)/cos(x(6)))**2)
      rosig=0.0023769*exp(beta*x(1))
      qa=0.5*rosig*x(4)**2*a
      phi=atan2(-(x(3)/cos(x(6))),-x(2))
      clnmax=2.0*w*nmax/(rosig*a*x(4)**2)
      if(x(8).lt.0.0) cl=-hfifi/(2.0*k*x(4)*x(8))
      if(x(8).ge.0.0) cl=clmax
      if(cl.gt.clmax) cl=clmax
      if(cl.gt.clnmax) cl=clnmax
      if(cl.lt.0.0) cl=0.0
      d=qa*(cdo+k*cl**2)
      mu2=0.0
      mu3=0.0
      if(t.lt.tc) go to 10
      pi=(d+w*sin(x(6))*(1.0-beta*x(4)**2/2.0/g))/tmax
      mu3=-x(8)
      go to 30
      if(cl.eq.clnmax.and.t.lt.tc.and.xi4.gt.x(4))
     &mu2=2.0*k*x(8)*clnmax+hfifi/x(4)
   10 if(x(8).eq.0.0) go to 20
      if(x(8).lt.0.0) pi=1.0
      if(x(8).gt.0.0) pi=-0.5
      go to 30
   20 if(xi4.gt.x(4)) f10=-(1.0/x(4)+x(5)*sin(x(6)))
      if(xi4.lt.x(4)) f10=2.0*g*hfifi*nmax/x(4)**2-
     &(1.0/x(4)+x(5)*sin(x(6)))
      if(f10.gt.0.0) pi=1.0
      if(f10.lt.0.0) pi=-0.5
   30 return
      end
```

```
      subroutine ndmiss(x,xi,r,rnorm)
      dimension x(10),xi(10),r(4)
      r(1)=(x(1)@xi(1))
      r(2)=(x(6)@xi(6))*57.29577951*10.0
      r(3)=(x(7)@xi(7))*57.29577951*10.0
      r(4)=(x(4)@xi(4))
      rnorm=0.0
      do 10 i=1,4
   10 rnorm=rnorm+r(i)*r(i)
      rnorm=sqrt(rnorm)
      return
      end
```

```
subroutine deltas(x,dx,tfs,tcs,lflag,ii,iii)
dimension x(10),dx(4)
dx(1)=x(1)*1.0e+05
dx(2)=x(2)*1.0e+04
dx(3)=tfs*1.0e+03
if(lflag.eq.2) dx(3)=x(3)*1.0e+04
dx(4)=tcs*1.0e+03
if(ii.eq.1.or.ii.eq.2) x(ii)=x(ii)+iii*dx(ii)
if(ii.eq.3.and.lflag.ne.2) tfs=tfs+iii*dx(3)
if(ii.eq.3.and.lflag.eq.2) x(3)=x(3)+iii*dx(3)
if(ii.eq.4) tcs=tcs+iii*dx(4)
return
end
```

```
      subroutine mtxinv(a,b,c,n)
      dimension a(n,n),b(n,n),c(n,n)
      do 5 i=1,n
      do 5 j=1,n
  5   c(i,j)=a(i,j)
      do 10 i=1,n
      do 10 j=1,n
 10   b(i,j)=0.0
      do 15 i=1,n
 15   b(i,i)=1.0

      do 35 i=1,n
      cstor1=c(i,i)
      do 20 j=1,n
      c(i,j)=c(i,j)/cstor1
 20   b(i,j)=b(i,j)/cstor1
      j=0
 25   j=j+1
      if(j.eq.i.and.i.eq.n) go to 40
      if(j.eq.i) j=j+1
      cstor2=c(j,i)
      do 30 k=1,n
      c(j,k)=c(j,k)-cstor2*c(i,k)
 30   b(j,k)=b(j,k)-cstor2*b(i,k)
      if(j.ne.n) go to 25
 35   continue
 40   return
      end
```
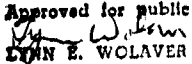
```fortran
      subroutine search(xf,xi,tf,tc,dz,r,rnorm,lflag,iprint)
      dimension xf(10),xi(10),x(10),r(4),rp(4),rm(4),dz(4)
      iter=0
      choice=0
      rnormm=9999999999.
      step1=1.0
      step2=0.618033989
      iterat=0
      mflag=0
    1 iter=iter+1
      gsr=step1*step2**(iter+1+iterat)
      write(5,*) iter,gsr
      do 2 j=1,2
    2 x(j)=xf(j)+gsr*dz(j)
      if(lflag.eq.2) x(3)=xf(3)+gsr*dz(3)
      do 3 j=5,10
    3 x(j)=xf(j)
      tfs=tf
      if(lflag.eq.1.or.lflag.eq.3) tfs=tf+gsr*dz(3)
      tcs=tc+gsr*dz(4)
      if(tcs.gt.tfs) tcs=tfs
      if(tcs.lt.0.0) tcs=0.0
      call assign(x,xi,tf,lflag)
      call integ(10,x,tfs,tcs,1)
      call ndmiss(x,xi,rp,rnormp)
      if(mflag.eq.1) go to 4
      if(rnormp.lt.(1.25*rnorm)) mflag=1
      if(mflag.eq.0) go to 4
      step1=gsr
      step2=0.618033989
      iterat=iter+1
    4 write(5,5) tfs,tcs,rp,rnormp
    5 format(1x,'tfs,tcs,rp,rnormp',/,7(1x,f10.4))
      if(rnormp.gt.rnormm) go to 7
      do 6 i=1,4
    6 rm(i)=rp(i)
      if(rnormp.lt.rnorm) rnormm=rnormp
    7 tcsave=tcs
      if(iter.lt.20) go to 1
      tc=tcsave
      if(tc.gt.tf) tc=tf
      if(tc.lt.0.001) tc=0.001
      call assign(xf,xi,tf,lflag)
      do 170 i=1,4
  170 r(i)=rm(i)
      rnorm=rnormm
      return
      end
```

VITA

Steven B. Dron was born on 29 Aug 1955 in Whittier, California. He graduate from Whittier Wiron High School in 1973 and then attended Northrop University from 1973 to 1977. Upon graduation he received the degree of Bachelor of Science in Aerospace Engineering and was commissioned in the USAF through the ROTC program. He entered the School of Engineering, Air Force Institute of Technology in September 1977 and was then transferred in December 1978 to the Flight Dynamics Laboratory, Air Force Wright Aeronautical Laboratories, where he was an Integrated Flight/Fire/Propulsion Control (IFFPC) Engineer and was the Laboratory Flight Control Evaluator for the DARPA Forward Swept Wing (FSW) Demonstrator program. In July 1981, he was transferred to the Space Defense Directorate, Space Division, Los Angeles AFS where he is currently the Anti-Satellite Flight Planning and Performance Branch Chief. Since his separation from AFIT in 1978, he has continued research to support completion of his thesis.

REPORT DOCUMENTATION PAGE

1a. REPORT SECURITY CLASSIFICATION UNCLASSIFIED		1b. RESTRICTIVE MARKINGS	
2a. SECURITY CLASSIFICATION AUTHORITY		3. DISTRIBUTION/AVAILABILITY OF REPORT Approved for public release; distribution unlimited	
2b. DECLASSIFICATION/DOWNGRADING SCHEDULE			
4. PERFORMING ORGANIZATION REPORT NUMBER(S) AFIT/GAE/AA/78D-5		5. MONITORING ORGANIZATION REPORT NUMBER(S)	
6a. NAME OF PERFORMING ORGANIZATION School of Engineering	6b. OFFICE SYMBOL (If applicable) AFIT/AA	7a. NAME OF MONITORING ORGANIZATION	
6c. ADDRESS (City, State and ZIP Code) Air Force Institute of Technology Wright-Patterson AFB, Ohio, 45433		7b. ADDRESS (City, State and ZIP Code)	
8a. NAME OF FUNDING/SPONSORING ORGANIZATION	8b. OFFICE SYMBOL (If applicable)	9. PROCUREMENT INSTRUMENT IDENTIFICATION NUMBER	

8c. ADDRESS (City, State and ZIP Code)	10. SOURCE OF FUNDING NOS.			
	PROGRAM ELEMENT NO.	PROJECT NO.	TASK NO.	WORK UNIT NO.
11. TITLE (Include Security Classification) See bolck 19				

12. PERSONAL AUTHOR(S) Steven B. Dron, B.S., Capt, USAF

13a. TYPE OF REPORT MS Thesis	13b. TIME COVERED FROM _____ TO _____	14. DATE OF REPORT (Yr., Mo., Day) 1984 September	15. PAGE COUNT 84
16. SUPPLEMENTARY NOTATION (cont f, p 86)			

17.	COSATI CODES		18. SUBJECT TERMS (Continue on reverse if necessary and identify by block number) Optimization Techniques; Minimum Time Turns; Optimal Controls; Singular controls , and
FIELD	GROUP	SUB. GR.	

19. ABSTRACT (Continue on reverse if necessary and identify by block number)

Title: HIGH SPECIFIC POWER AIRCRAFT TURN MANEUVERS: TRADEOFF OF TIME-TO-TURN

VERSUS CHANGE IN SPECIFIC ENERGY

Thesis Chairman: Dr. James E. Rader, Major, USAF

Approved for public release: IAW AFR 190-17.

LYNN E. WOLAVER   25 Feb 85
Dean for Research and Professional Development
Air Force Institute of Technology (ATC)
Wright-Patterson AFB OH 45433

20. DISTRIBUTION/AVAILABILITY OF ABSTRACT CLASSIFIED/UNLIMITED ☒ SAME AS RPT. ☐ DTIC USERS ☐	21. ABSTRACT SECURITY CLASSIFICATION UNCLASSIFIED	
22a. NAME OF RESPONSIBLE INDIVIDUAL Dr. Peter J. Torvik	22b. TELEPHONE NUMBER (Include Area Code) (513)-255-2109	22c. OFFICE SYMBOL AFIT/ENY

DD FORM 1473, 83 APR   EDITION OF 1 JAN 73 IS OBSOLETE.   UNCLASSIFIED

UNCLASSIFIED

SECURITY CLASSIFICATION OF THIS PAGE

This thesis   *deg*

The report deals with the tradeoff between time-to-turn and the change in specific
energy during a turn of 180°, for an aircraft of high specific power. This type of
aircraft possesses the capability to sustain flight at the corner velocity where both
maximum lift coefficient and maximum load factor occur simultaneously. However, the
classical necessary conditions breakdown on this corner velocity arc and an additional
constraint must be defined to determine the optimal control histories. The report
first defines the necessary conditions for a generic optimal control formulation and
then applies the formulation to this high specific power aircraft problem. The result
is a three-point boundary value problem with a discontinuous interior corner condition
at the beginning of the sustained corner velocity arc. All state and costate derivatives
and end conditions are presented with numerical methods for determining both minimum
time and maximum energy gradient solutions. Anticipated results are provided for the
formulations beginning at initial conditions both above and below the corner velocity.
Results are presented for the minimum time solution only. Recommendations for further
work in this same area are also provided.
Originator-supplied Keywords
include: